# Function and dynamics of PKD2 in *Chlamydomonas reinhardtii* flagella

Kaiyao Huang,[1] Dennis R. Diener,[1] Aaron Mitchell,[1] Gregory J. Pazour,[2] George B. Witman,[3] and Joel L. Rosenbaum[1]

[1]Department of Molecular Cell and Developmental Biology, Yale University, New Haven, CT 06520
[2]Program in Molecular Medicine, University of Massachusetts Medical School, Worcester, MA 01605
[3]Department of Cell Biology, University of Massachusetts Medical School, Worcester, MA 01655

To analyze the function of ciliary polycystic kidney disease 2 (PKD2) and its relationship to intraflagellar transport (IFT), we cloned the gene encoding *Chlamydomonas reinhardtii* PKD2 (CrPKD2), a protein with the characteristics of PKD2 family members. Three forms of this protein (210, 120, and 90 kD) were detected in whole cells; the two smaller forms are cleavage products of the 210-kD protein and were the predominant forms in flagella. In cells expressing CrPKD2–GFP, about 10% of flagellar CrPKD2–GFP was observed moving in the flagellar membrane. When IFT was blocked, fluorescence recovery after photobleaching of flagellar CrPKD2–GFP was attenuated and CrPKD2 accumulated in the flagella. Flagellar CrPKD2 increased fourfold during gametogenesis, and several *CrPKD2* RNA interference strains showed defects in flagella-dependent mating. These results suggest that the CrPKD2 cation channel is involved in coupling flagellar adhesion at the beginning of mating to the increase in flagellar calcium required for subsequent steps in mating.

## Introduction

Polycystin-2, also known as TRPP2, is a member of the transient receptor potential (TRP) family of channels that are present in organisms from yeast (Palmer et al., 2005) to humans (Mochizuki et al., 1996; Barr and Sternberg, 1999; Gao et al., 2003; Watnick et al., 2003; Sun et al., 2004). Characteristic of TPR channels, polycystin-2 contains six transmembrane domains and functions as a $Ca^{2+}$-permeable, nonselective cation channel (Mochizuki et al., 1996; Hanaoka et al., 2000; Luo et al., 2003; Tsiokas et al., 2007). This channel is found predominantly in the ER, but also in the basolateral plasma membrane, mitotic spindles (Torres and Harris, 2006), and, notably, primary cilia (Pazour et al., 2002; Yoder et al., 2002). Polycystin-2 is of particular interest because mutations affecting it or polycystin-1, with which it interacts, are the primary cause of autosomal dominant polycystic kidney disease (PKD), a genetic disorder characterized by the formation of cysts, particularly in the ducts of the kidney and liver (Gabow, 1993; Torres and Harris, 2006).

Polycystin-2 located on primary cilia in the kidney is a pivotal factor in the etiology of PKD. The first clue linking PKD and cilia came from the characterization of intraflagellar transport (IFT) subunits in *Chlamydomonas reinhardtii* (Cole et al., 1998). IFT is a transport mechanism responsible for the assembly and maintenance of eukaryotic flagella (Kozminski et al., 1993; Rosenbaum and Witman, 2002; Scholey, 2003). The IFT machinery consists of the anterograde motor kinesin-2, the retrograde motor dynein 1b (dynein 2 in mammals), and IFT particles comprised of ~17 proteins. These IFT components are conserved in organisms with cilia including humans, mice, zebrafish, *Drosophila melanogaster*, and *Caenorhabditis elegans* (Cole, 2003; Avidor-Reiss et al., 2004; Li et al., 2004). The link between PKD and cilia emerged when the mouse homologue of one IFT subunit, IFT88, was found to be encoded by *Tg737* (Pazour et al., 2000), a gene previously shown to cause kidney defects very similar to those seen in humans with autosomal recessive PKD (Moyer et al., 1994). The tie between PKD and cilia became clearer as homologues of polycystin-1 and -2 were found on the cilia of sensory neurons of *C. elegans* (Barr and Sternberg, 1999) and the primary cilia of mouse kidney (Pazour et al., 2002; Yoder et al., 2002). These and subsequent studies have shown that almost all the proteins associated with the PKD phenotype (polycystin-1, polycystin-2, fibrocystin, nephrocystins, inversin, cystin, IFT88/polaris/Tg737, and Bardet-Biedl syndrome proteins) are present on cilia (Davenport and Yoder, 2005).

Understanding the importance of cilia in maintaining homeostasis of the kidney has stimulated the study of the sensory

Correspondence to J.L. Rosenbaum: joel.rosenbaum@yale.edu

Abbreviations used in this paper: CrPKD2, *Chlamydomonas reinhardtii* PKD2; DIC, differential interference contrast; FMG, flagellar membrane glycoprotein; IFT, intraflagellar transport; mt, mating type; NaPPi, sodium pyrophosphate; PKD, polycystic kidney disease; TRP, transient receptor potential; UTR, untranslated region.

The online version of this paper contains supplemental material.


The Journal of Cell Biology, Vol. 179, No. 3, November 5, 2007 501–514
http://www.jcb.org/cgi/doi/10.1083/jcb.200704069

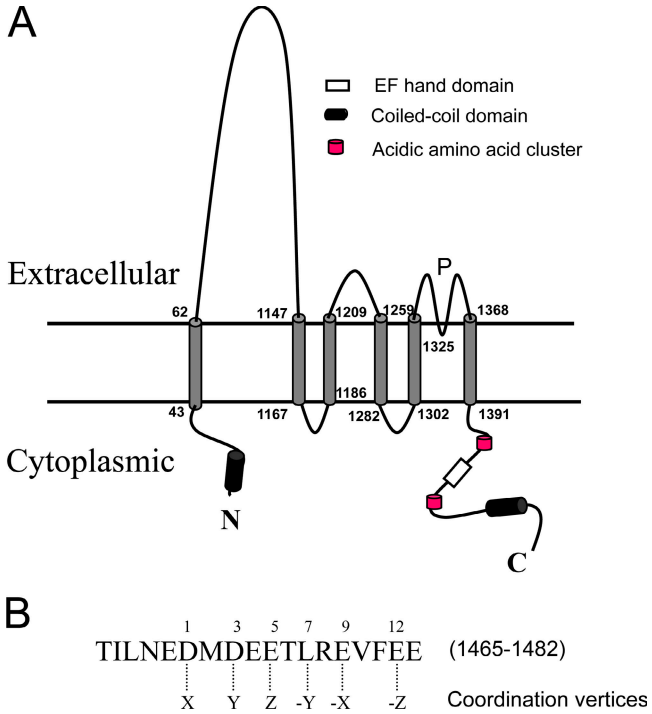


Figure 1. **CrPKD2 is a member of the TRPP2 family.** (A) Secondary structure of CrPKD2. CrPKD2 contains a coiled-coil domain at the N and C termini, an EF hand domain, six transmembrane domains (numbers denote amino acid positions), and acidic amino acid cluster domains. The pore region (P) is shown, between aa 1,342–1,377, by comparison to human and *D. melanogaster* PKD2 (Tsiokas et al., 1999; Venglarik et al., 2004). Not drawn to scale. (B) The EF hand domain of CrPKD2 contains the six conserved residues (coordination vertices) involved in calcium binding (positions 1, 3, 5, 7, 9, and 12).

function and signaling pathways of kidney cilia. These studies support a model in which polycystin-1 and -2 comprise a mechanosensory complex that translates deflection of the cilium into signals associated with the control of the cell cycle (Torres and Harris, 2006). Ciliary bending results in an increase in intracellular $Ca^{2+}$ (Praetorius and Spring, 2001) that is dependent on polycystin-1 and -2 (Nauli et al., 2003). In the absence of fluid flow and ciliary bending, the C terminus of polycystin-1 is cleaved and moves to the nucleus, where it activates signaling pathways known to be involved in cell cycle control (Chauvet et al., 2004; Low et al., 2006). How the signals generated by ciliary PKD2 are transferred to the cell body and whether the many PKD-related proteins located in the cilium interact with PKD1 and 2 to participate in signal transduction is unclear.

Most studies of PKD have been performed in mice, vertebrate kidney cell lines in culture, or the nonmammalian model *C. elegans* (Barr and Sternberg, 1999; Ong and Harris, 2005). In none of these systems is it practical to isolate sufficient cilia for biochemical analysis. For this reason we chose to work on polycystin-2 in the biflagellate alga *C. reinhardtii*, where biochemical quantities of cilia can be easily isolated. This organism also has excellent, well-established genetics to complement the biochemistry, as well as a sequenced genome and proteomic data from both the cilia and basal bodies (Keller et al., 2005; Pazour et al., 2005). Furthermore, *C. reinhardtii* homologues of polycystin-2 and other PKD-related proteins were identified by comparative genomic and flagellar proteomic analyses (Li et al., 2004; Pazour et al., 2005). In this paper, we cloned a *C. reinhardtii* gene encoding a member of the PKD2 family. The protein is cleaved in the cell body before entering flagella and is enriched in the flagellar membrane. Most of the *C. reinhardtii* PKD2 (CrPKD2) remains static in the flagella, but a fraction (<10%) moves at a rate similar to IFT. RNAi knockdown of CrPKD2 results in a decrease in the efficiency of mating, a process initiated by the contact of flagella of gametes of opposite mating types (mts), which activates a calcium signaling pathway required for the fusion of the gametes. These observations provide new insights into the function and dynamics of PKD2 in cilia.

## Results

### PKD2 homologue in *C. reinhardtii*

A predicted protein in the *C. reinhardtii* genome sequence database (C_590099 in assembly two) showed significant similarity to human polycystin-2 ($e = 6 \times 10^{-11}$), and 10 peptide fragments of this protein were found in the flagellar proteome (Pazour et al., 2005). The available EST clones corresponding to this protein (Asamizu et al., 1999) were sequenced, and one, AV395567, encoded most of the protein as well as the 3′ untranslated region (UTR), including a polyadenylation signal (TGTAA) typical for a *C. reinhardtii* gene. No EST clone encoded the putative transcriptional start site of this gene, so several sets of primers were designed based on genomic sequence to be used for RT-PCR. According to the sequence of these PCR products, the cDNA begins 410 bp upstream from the transcriptional site predicted by the C_590099 gene model (the cDNA sequence is available from GenBank/EMBL/DDBJ under accession no. EF446617). The *CrPKD2* gene (Fig. S1 A, available at http://www.jcb.org/cgi/content/full/jcb.200704069/DC1) encodes a protein of 1,626 aa (Fig. S1 B) with a molecular mass of 181 kD and a theoretical isoelectric point of 4.86.

A comparison of the predicted gene product with a variety of TRP channels shows that it clusters with the TRPP subfamily (Fig. S2, available at http://www.jcb.org/cgi/content/full/jcb.200704069/DC1) and exhibits the signatures typical of PKD2: it has six transmembrane domains that show homology to ion transport proteins, a coiled-coil domain at the C terminus, and an EF hand domain (Fig. 1 A). The six residues in the CrPKD2 sequence predicted to coordinate $Ca^{2+}$ binding in the EF hand (positions 1, 3, 5, 7, 9, and 12) are allowable (Fig. 1 B): X (D), Y (DNS), Z (DENSTG), −Y {GP}, −X (DENQSTAGC), and −Z (DE) (CrPKD2 residues are underlined; Prosite documentation PDOC00018). Moreover, the C terminus of CrPKD2 contains two acidic clusters; one has the casein kinase II phosphorylation motif (EGDDKDDSPEVREE), where S is the phosphorylation site predicted by NetPhosK 1.0 (http://www.cbs.dtu.dk/services/NetPhosK/), and the other one does not (DEDEDDD; Figs. 1 A and S1). Acidic clusters bind phosphofurin acidic cluster sorting proteins, which are involved in routing PKD2 between the ER, Golgi apparatus, and plasma membrane in mammalian cells (Kottgen et al., 2005). Because acidic clusters are characteristic of mammalian PKD2, but not PKD2-like proteins

(Kottgen et al., 2005), CrPKD2 may be an orthologue of PKD2; however, this trait alone cannot unambiguously distinguish CrPKD2 from other PKD2 family members (i.e., PKD2L1 and PKD2L2). In addition, the casein kinase II phosphorylation site that controls targeting and function of PKD2 in the sensory cilia of *C. elegans* (Hu et al., 2006) is also present in CrPKD2.

Unlike other PKD2s, however, CrPKD2 is predicted to have a coiled-coil domain at its N terminus. Another distinguishing characteristic of CrPKD2 is that its first extracellular loop is atypically long (1,085 aa). Whereas two subfamilies of TRP channels, TRPP and TRPML, have an extracellular loop between the first two transmembrane domains, this loop is typically only ~200 aa residues long (Montell, 2005).

### CrPKD2 is cleaved

Two polyclonal antibodies were generated against CrPKD2. One antibody (L1-PKD2) was directed against the first predicted loop (aa 358–1,019) expressed in *Escherichia coli* (Fig. 2 A) and the other (C-PKD2) was generated against a C-terminal peptide (aa 1,444–1,462). Immunoblots of whole cells probed with the L1-PKD2 revealed three proteins of 210, 120, and 90 kD (Fig. 2 B, lane 1). Only the two smaller fragments (120 and 90 kD) were present in flagella (Fig. 2 B, lane 2). The smaller forms of CrPKD2 do not appear to arise from alternate mRNA splicing because only one 6-kbp transcript, corresponding to the 210-kD form, hybridizes to *CrPKD2* probes (Fig. S3, available at http://www.jcb.org/cgi/content/full/jcb.200704069/DC1). When immunoblots were probed with C-PKD2, two forms, 210 and 90 kD, were detected in whole cells (Fig. 2 B, lane 3) and only the 90-kD form was seen in flagella (Fig. 2 B, lane 4). C-PKD2 did not recognize the 120-kD protein, suggesting that this species lacks the C terminus. The simplest explanation of the multiple forms of CrPKD2 is that posttranslational cleavage of 210-kD full-length CrPKD2 produces a 120-kD N-terminal fragment and a 90-kD C-terminal fragment. The epitope recognized by L1-PKD2 spans the cleavage site, so this antibody recognizes both fragments, whereas the C-PKD2 epitope is unique to the C-terminal fragment (Fig. 2 A). To test this explanation, an N-terminal peptide of the first loop (aa 358–583) was used to affinity purify an antibody from the L1-PKD2 antiserum. This antibody (N-PKD2) was predicted to only react with the 210- and 120-kD forms of CrPKD2. As expected, only these two bands were seen in immunoblots of whole cells and only the 120-kD band appeared in flagella (Fig. 2 B, lanes 5 and 6).

The identities of the 210- and 90-kD bands were further corroborated by tagging the C terminus of CrPKD2 with GFP and expressing the fusion protein in *C. reinhardtii* along with endogenous CrPKD2. Probing immunoblots of cells expressing CrPKD2–GFP with an antibody against GFP revealed two bands of 240 and 120 kD (Fig. 2 C, lane 1). These represent the 210-kD full-length CrPKD2 plus the 30-kD GFP tag and the 90-kD C-terminal fragment plus the 30-kD GFP tag. Only the 120-kD band was present in flagella (Fig. 2 C, lane 2). The identity of the GFP-tagged bands in whole cells was confirmed with the C-PKD2 antibody, which detected both GFP-tagged bands along with the two endogenous untagged forms (Fig. 2 C, lane 3). These data fit the model that the 210-kD initial CrPKD2 product is

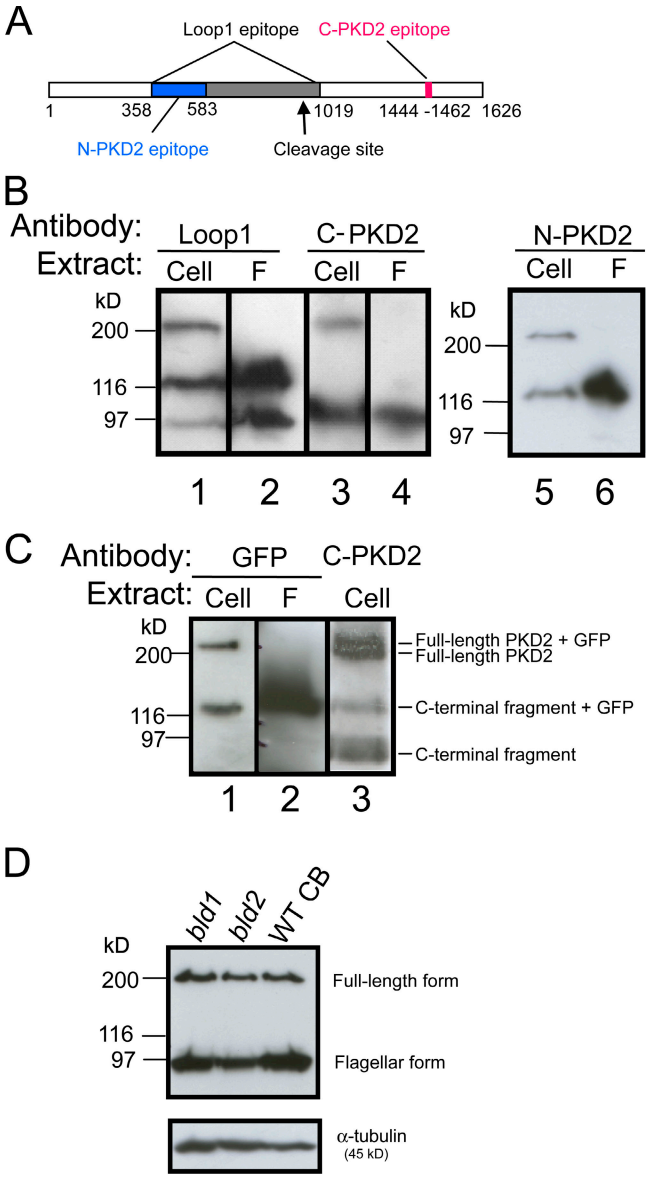


Figure 2. **Flagellar CrPKD2 is cleaved.** (A) Diagram of the CrPKD2 protein showing the regions used to generate the Loop1 and N- and C-terminal antibodies. The arrow marks the approximate location of the CrPKD2 cleavage site that generates fragments of 120 and 90 kD. (B) Immunoblots from whole cells (Cell) and flagella (F) of wild-type cells were probed with antibodies against Loop1 or the N or C termini of CrPKD2. The Loop1 antibody reacts with three bands (210, 120, and 90 kD; lane 1) in whole cells, but only the smaller two bands are present in flagella (lane 2). The C-terminal antibody does not react with the 120-kD N-terminal fragment (lanes 3 and 4), demonstrating that this fragment does not include the C terminus of the protein. The N-terminal antibody reacts with two bands (210 and 120 kD) in whole cells and the 120-kD form in the flagella (lanes 5 and 6). Thus, full-length CrPKD2 is cleaved into two fragments (120 and 90 kD) that are present in flagella. (C) Immunoblot of transformant expressing CrPKD2–GFP. GFP-tagging results in two bands that react with the GFP antibody (lane 1): a 240-kD band (the 210-kD full-length PKD2 + 30 kD GFP) and a 120-kD band (the 90-kD C-terminal fragment + 30 kD GFP). Only the smaller band is present in flagella (lane 2). Both bands also react with the C-PKD2 antibody (lane 3), as do the untagged CrPKD2 bands also present in these cells. (D) Immunoblots of *bld1* and *bld2* cells (mutants that have no flagella) and cell bodies of wild-type cells (WT CB) probed with the anti–C-PKD2 antibody. The flagellar form of CrPKD2 is present in the cell bodies, indicating that cleavage occurs in the cell body. The same blot was probed with α-tubulin as a loading control.

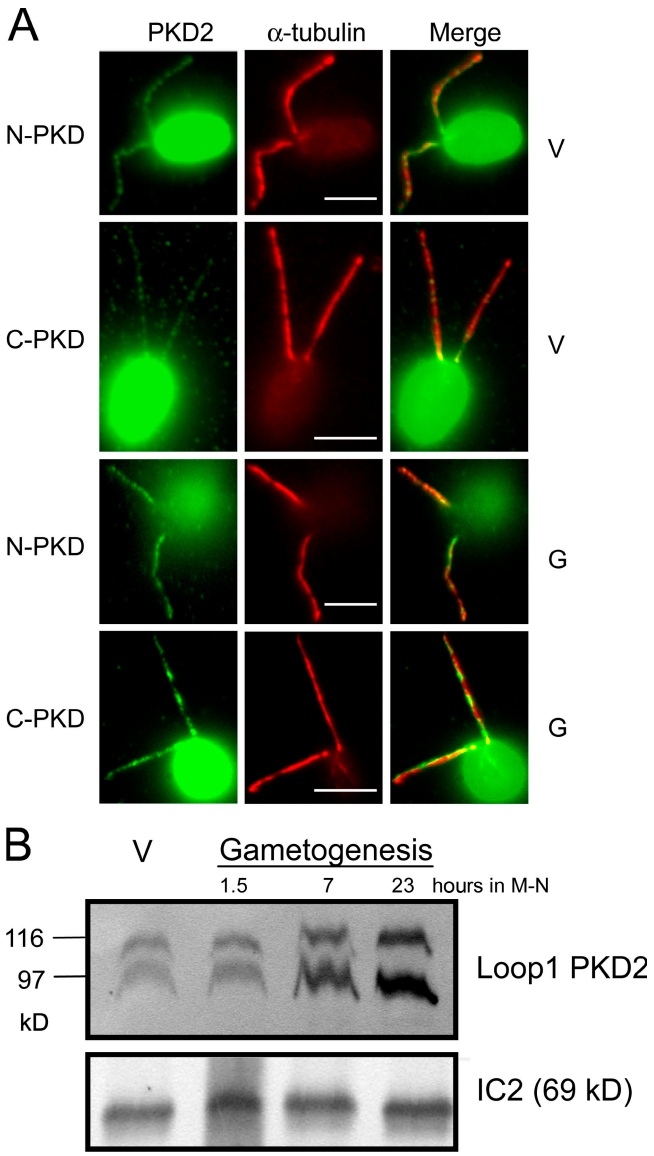


Figure 3. **Flagellar CrPKD2 increases during gametogenesis.** (A) *C. reinhardtii* vegetative cells (V) and gametes (G) stained with N-PKD2 or C-PKD2 (green) and acetylated α-tubulin (red) antibodies. Bars, 5 μm. (B) 10 μg of flagellar protein from CC125 (mt+) vegetative cells and cells undergoing gametic differentiation in nitrogen-deficient medium was probed on immunoblots with antibodies against the Loop1 PKD2 epitope and an intermediate chain of outer arm dynein, IC2, as a loading control. The amount of CrPKD2 in the flagella increased during the course of gametic differentiation.

cleaved near the C end of the first extracellular loop (aa 583–1,019) to produce a 120-kD N-terminal fragment and a 90-kD C-terminal fragment. A more detailed examination of immunoblots of the CrPKD2–GFP cells is presented in Fig. S4 (available at http://www.jcb.org/cgi/content/full/jcb.200704069/DC1). Further evidence that the 210-, 120-, and 90-kD bands are all derived from CrPKD2 came from analysis of CrPKD2 RNAi knockdown strains, in which the levels of all three bands were reduced (see Function of CrPKD2 in the mating of *C. reinhardtii*).

To determine whether the cleavage occurs in the cell body or flagella, we isolated extracts from *bld1* cells, which have only short flagellar stubs because of a mutation in the gene encoding IFT52, a component of IFT complex B (Brazelton et al., 2001; Deane et al., 2001), and *bld2* cells, which form basal bodies consisting of microtubule singlets instead of triplets because of a deficiency in ε-tubulin (Dutcher et al., 2002). These aberrant basal bodies do not attach to the cell surface, form transitional fibers, nor nucleate flagellar microtubules (Dutcher et al., 2002). We also isolated extracts from wild-type cell bodies, i.e., cell bodies from which the flagella had been detached. Both full-length and cleaved CrPKD2 were present in *bld1*, *bld2*, and wild-type cell bodies (Fig. 2 D), indicating that CrPKD2 can be cleaved in the cell body before entering the flagella.

### CrPKD2 is located in the flagellar membrane

When *C. reinhardtii* cells were stained with the N-PKD2 or C-PKD2 antibody, CrPKD2 was detected both in the cell body and flagella of vegetative cells and gametes (Fig. 3 A). No difference was detected in the distribution of CrPKD2 with the two antibodies. Immunoblot analysis of the flagella of cells undergoing gametogenesis showed that a fourfold increase in the amount of CrPKD2 gradually occurred during gametic differentiation induced when cells are starved for nitrogen (Fig. 3 B).

In the flagellar proteomic analysis, most of the CrPKD2 peptides were obtained from the axonemal fraction rather than the membrane and matrix fraction (Pazour et al., 2005). This was an unexpected result for a transmembrane protein, which raised the possibility that CrPKD2 might be a membrane protein tethered to the axonemal microtubules. To investigate this further, we developed methods for the isolation and purification of flagellar membranes. Membranes were released from isolated flagella with 0.1% NP-40 (4°C for 30 min), and the axonemes were removed by centrifugation. The resultant membrane and matrix fraction contained membrane vesicles in addition to soluble flagellar proteins. Membranes either were sedimented directly from the membrane and matrix fraction to recover all the membranes present or further purified by density gradient centrifugation using Optiprep to obtain a band of uniform density (see Materials and methods). EM (Fig. 4 A) and SDS-PAGE analysis (Fig. 4 B) of the resultant membrane fractions showed they contained little axonemal contamination and were enriched in the major flagellar membrane glycoprotein (FMG) 1 (Bloodgood et al., 1986). CrPKD2 was concentrated in the flagellar membrane fraction (Fig. 4 B), confirming that it is a membrane protein. Interestingly, IFT proteins also were found in these membrane fractions.

Because some CrPKD2 remained on the axonemes after detergent extraction, we used more stringent conditions in an attempt to solubilize more CrPKD2. Freezing flagella in liquid nitrogen and thawing releases the matrix and a small amount of membrane, but much of the membrane remains in the axonemal pellet (not depicted). Such axonemes were extracted twice with 0.1 or 1% NP-40 at room temperature for 30 min, and after low speed centrifugation, the soluble fraction contained the membrane and the pellet contained the axonemes. No vesicles or other membrane remained associated with the axonemes after extraction in 1% NP-40 (Fig. 4 D), and all the membrane

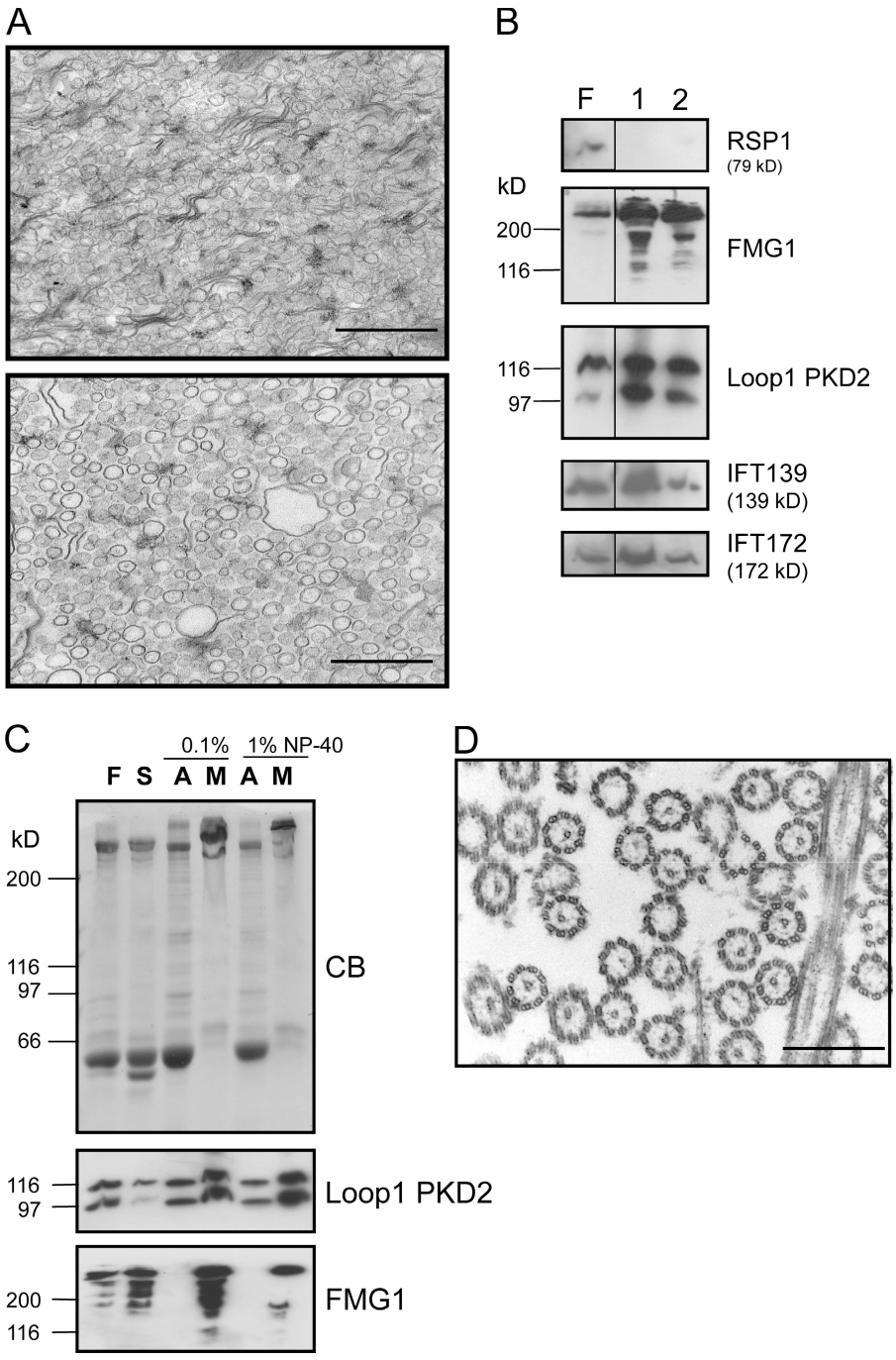


Figure 4. **CrPKD2 is concentrated in flagellar membranes.** (A) Electron micrographs of thin sections of isolated flagellar membrane vesicles. Flagellar membranes were isolated in 0.1% NP-40 and were sedimented (top) or further purified on an Optiprep gradient (bottom). (B) Immunoblots of the proteins (2.3 μg) in flagella (F) and vesicles from A purified without (1) or with (2) an Optiprep gradient were probed for an axonemal protein radial spoke protein 1, FMG-1, Loop1 PKD2, IFT 139 (IFT complex A), and IFT172 (IFT complex B). Black lines indicate that intervening lanes have been spliced out. (C) Coomassie blue–stained gel (CB) of equal protein loadings (11 μg) of flagellar fractions and immunoblots probed with FMG-1 and Loop1 PKD2 antibodies. FMG-1 and CrPKD2 are concentrated in flagellar membrane fractions. Some CrPKD2 remains associated with the axoneme even though the FMG-1 is released from the axoneme completely. F, flagella; S, flagellar proteins solubilized by freeze–thaw; A, axoneme extracted with 0.1 or 1% NP-40; M, corresponding flagellar membrane. (D) Electron micrograph of axonemes extracted with 1% NP-40 from Fig. 4 C. Bars: (A) 50 nm; (D) 500 nm.

glycoprotein FMG-1 was released (Fig. 4 C); however, 20–25% of the CrPKD2 still remained in the axonemal fraction. Thus, these two membrane proteins show different patterns of solubilization in the flagella: FMG-1 is completely released by nonionic detergent, whereas flagellar CrPKD2 is present in two pools, one that is easily released by nonionic detergent and one that is not.

### Movement of flagellar CrPKD2

To examine the movement of CrPKD2 in the flagellum, we made a construct designed to express CrPKD2 fused to GFP via a flexible linker of 10 aa. After transformation of cells with the construct, the fluorescence of PKD–GFP was detected in flagella. Like the immunofluorescence localization of CrPKD2 (Fig. 3 A), flagellar CrPKD2–GFP was concentrated in puncta (Fig. 5 A), which may represent clustered channels. When visualized by time-lapse imaging, $<10\%$ of the PKD–GFP particles moved continuously to the tip of the flagella at a velocity of $\sim$1.6 μm/s, even though most of the puncta did not move (Fig. 5 and Video 1, available at http://www.jcb.org/cgi/content/full/jcb.200704069/DC1). Movement of CrPKD2– GFP toward the base was not detected, perhaps because the faint fluorescence of CrPKD2–GFP was bleached as the protein moved to the tip and became too faint to see as it returned to the cell body.

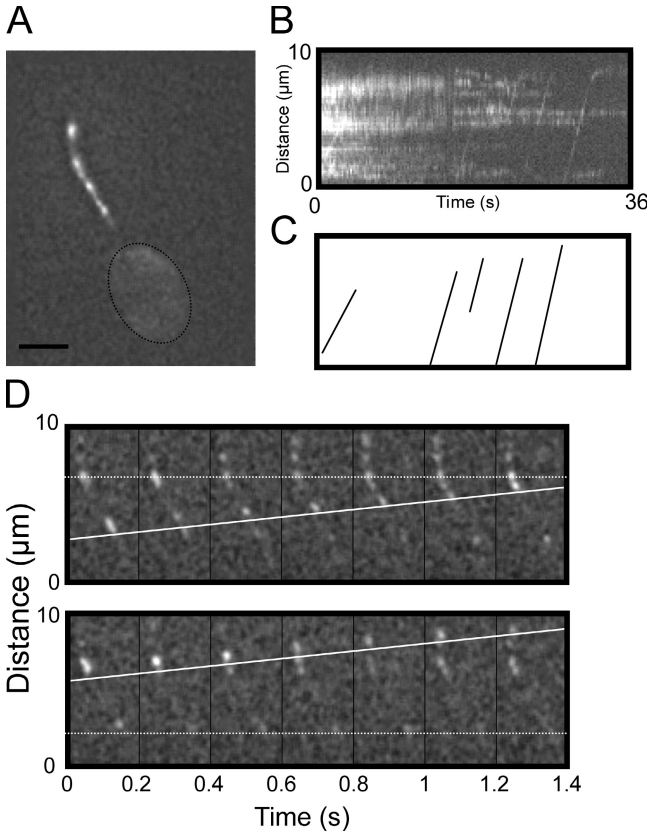


Figure 5. **Some of the CrPKD2–GFP moves in the flagellar membrane.** (A) Fluorescence micrograph of the flagellum used to generate the kymographs of CrPKD2–GFP. Only one flagellum was illuminated. The cell body is outlined with a dotted line. (B) Kymograph of CrPKD2–GFP generated using the video (Video 1, available at http://www.jcb.org/cgi/content/full/jcb.200704069/DC1). (C) The lines corresponding to those seen in the kymograph were used to measure the anterograde velocity of CrPKD2–GFP. (D) Two CrPKD2–GFP particles are shown (above the solid line) moving in the anterograde direction at ~1.6 μm/s. The dotted lines mark particles that did not move.

To assay the movement of CrPKD2–GFP in the absence of IFT, we generated a strain that expressed CrPKD2–GFP in a *fla10* background. Because *fla10* is a temperature-sensitive mutant of the IFT anterograde motor, we could monitor CrPKD2–GFP movement in the presence and absence of IFT at permissive and restrictive temperatures, respectively. 50 videos were generated of *fla10* flagella at permissive and nonpermissive temperatures, and kymographs of these were analyzed for movement. In 10 sequences taken at permissive temperature, movement was observed; however, none was seen in flagella of cells incubated at 32°C. These results suggest the movement of visible puncta of CrPKD2 is dependent on IFT.

Movement of small puncta is difficult to detect in kymographic analysis of videos, so FRAP was used as a more sensitive assay for the effect of IFT on CrPKD2 movement. To this end, a 2-μm section in the center of a flagellum of *fla10* cells expressing CrPKD2–GFP was bleached at permissive temperature, the area was allowed to recover for 1 or 2 min without illumination, and the fluorescence intensity was measured again. The fluorescence recovered 10 and 19% of its original intensity after 1 and 2 min of recovery, respectively (Fig. 6, A and B). This result is consistent with the observation that most of the flagellar PKD remains stationary, whereas only a small fraction of it moves.

FRAP also was performed on *fla10* cells expressing CrPKD2–GFP at restrictive temperature. After 2 min of recovery, the fluorescence in the bleached region recovered only 9.4% at nonpermissive temperature (Fig. 6 B). The reduction of FRAP at 32°C was not simply a temperature effect, because no such reduction (Fig. 6 C) was seen in control *pf18* cells. The *pf18* cells were used because they have paralyzed flagella, facilitating measurement of CrPKD2 FRAP, but are not deficient in FLA10 or IFT (Dentler, 2005). These data suggest that IFT is important for the movement of CrPKD2–GFP in flagella, but because some recovery of fluorescence occurred in the absence of IFT, other mechanisms may be involved.

Further evidence for a role of IFT in the movement of CrPKD2 was obtained from biochemical analysis of the flagella of *fla10* cells after incubation at 32°C for 1 or 1.5 h in 10 mM Hepes, pH 7.2. At these times, IFT proteins were dramatically decreased (Fig. 7 A), no IFT particles could be observed moving by differential interference contrast (DIC) microscopy (Kozminski et al., 1995), and the flagella had shortened to about half length (Table S1, available at http://www.jcb.org/cgi/content/full/jcb.200704069/DC1). Under these conditions, the concentration of flagellar CrPKD2 increased relative to total flagellar protein (Fig. 7 A). To determine if this increase was caused by the absence of IFT or simply flagellar shortening, the amount of CrPKD2 was examined in flagella induced to shorten by the addition of sodium pyrophosphate (NaPPi; Lefebvre et al., 1978), which causes the flagella to shorten as IFT continues unabated (Dentler, 2005; Pan and Snell, 2005). In this case, the concentration of flagellar CrPKD2 did not change (Fig. 7 B) as the flagella shortened. Thus, flagellar shortening does not per se affect the concentration of flagellar CrPKD2 when IFT is functioning properly; however, when IFT is defective, the concentration of CrPKD2 in the flagella increases, perhaps because it cannot be removed from the flagella in the absence of IFT.

### Function of CrPKD2 in the mating of *C. reinhardtii*

The observation that CrPKD2 increases in the flagella of gametes (Fig. 3 B) suggests that CrPKD2 may have some function in the calcium-dependent steps of mating. The sexual cycle of *C. reinhardtii* begins with gametogenesis (Fig. 8 A). Vegetative (haploid) cells differentiate into gametes when they are starved for nitrogen. When gametes of mt+ and − strains are mixed, the flagella of gametes of opposite mts adhere to each other, mediated by mt-specific agglutinins on the flagellar membrane (Bergman et al., 1975). Flagellar adhesion is followed by a cascade of signaling events that result in the shedding of the cell wall, formation of mating structures on mt+ and − gametes, and ultimately cell fusion (Fig. 8 A; Pasquale and Goodenough, 1987; Quarmby, 1994; Pan and Snell, 2000; Wang et al., 2006). The early stages of this cascade are blocked by drugs that interfere with $Ca^{2+}$ signaling (Snell et al., 1982; Bloodgood and Levin, 1983; Goodenough et al., 1993), suggesting that an influx of $Ca^{2+}$ is required as an early step in mating. This influx is

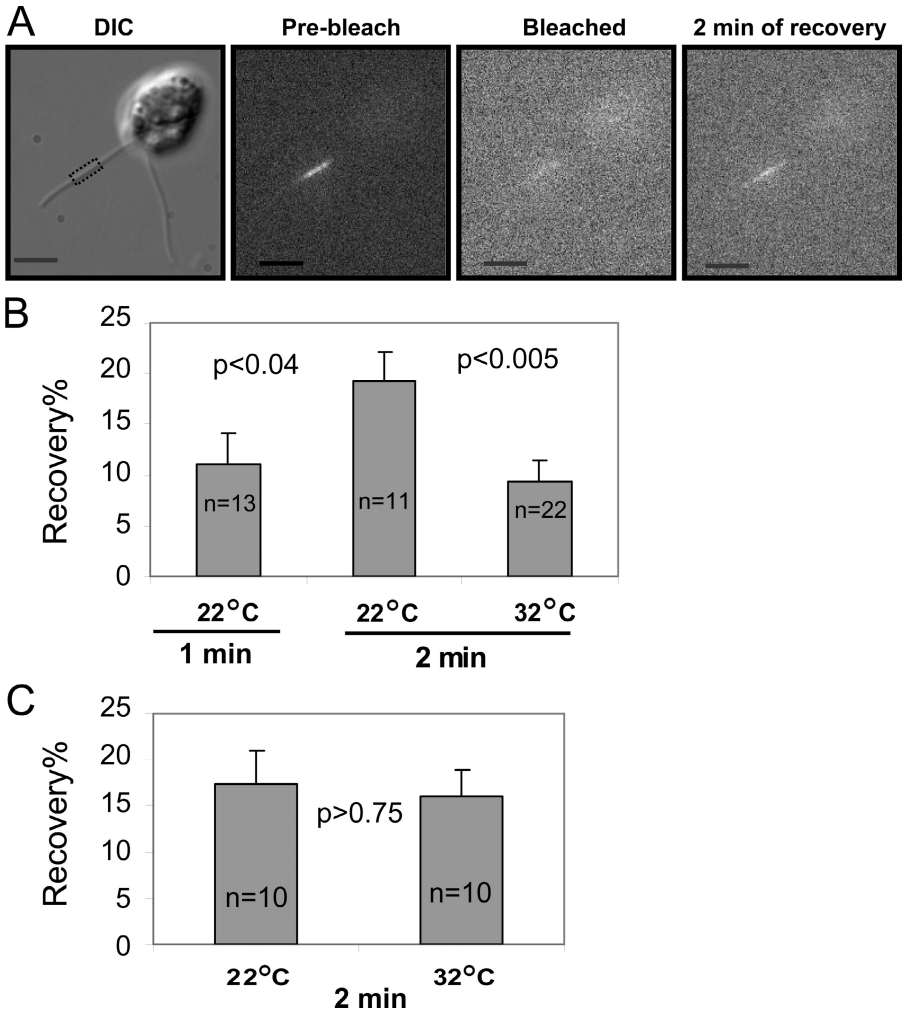


Figure 6. **CrPKD2–GFP FRAP is reduced in the flagella of *fla10* cells at restrictive temperature.** (A) An ~2-μm segment of a *fla10* flagellum containing CrPKD2–GFP is shown (box in DIC panel) before bleaching, after bleaching, and after 2 min of recovery. The rest of the flagellum is not visible because it is not illuminated. (B) The fluorescence in the bleached area increased in the flagellum of *fla10* cells at nonrestrictive temperature after 1 and 2 min after photobleaching. In *fla10* cells at restrictive temperature, recovery only reached 9.4 versus 19.3% at permissive temperature. (C) In control (*pf18*) cells at 22 and 32°C, fluorescence recovery is similar to that of *fla10* cells at room temperature. Bar graphs represent mean ± SEM (statistics determined by *t* test).

followed by the phosphorylation and activation of a cyclic GMP-dependent protein kinase (CrPKG), which in turn increases the concentration of flagellar cAMP by up-regulating an adenylate cyclase in the flagellar membrane (Fig. 8 B; Pasquale and Goodenough, 1987; Wang and Snell, 2003; Wang et al., 2006). Ultimately, the cAMP concentration in the cell body rises and the mt+ and − gametes elaborate mating structures that touch to initiate cell fusion.

We took advantage of RNAi to knockdown the endogenous CrPKD2 and examine the function of CrPKD2 in mating. The RNAi construct consisted of genomic CrPKD2 DNA including its native promoter with the corresponding cDNA in reverse orientation (Fig. 9 A). This strategy has been shown to efficiently knockdown endogenous proteins in *C. reinhardtii* (Fuhrmann et al., 2001; Huang and Beck, 2003). Transformants were obtained in which CrPKD2 was decreased to 10% of wild-type

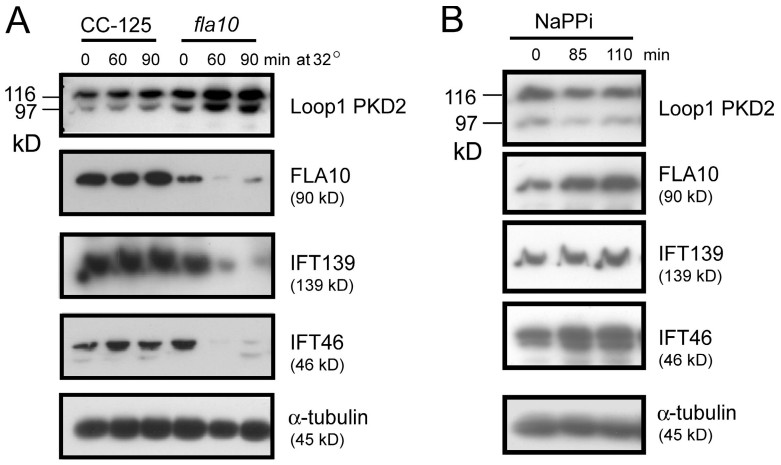


Figure 7. **Flagellar CrPKD2 increases when IFT is blocked.** (A) Wild-type and *fla10* cells were shifted to 32° for 1 or 1.5 h, and immunoblots of isolated flagella were probed with antibodies as listed. Note the rise in CrPKD2 when IFT proteins disappear in flagella from *fla10* cells. (B) Cells were treated with 20 mM NaPPi to induce flagellar resorption, and flagellar proteins were probed on immunoblots as in A. CrPKD2 did not increase in these flagella during resorption under this condition.

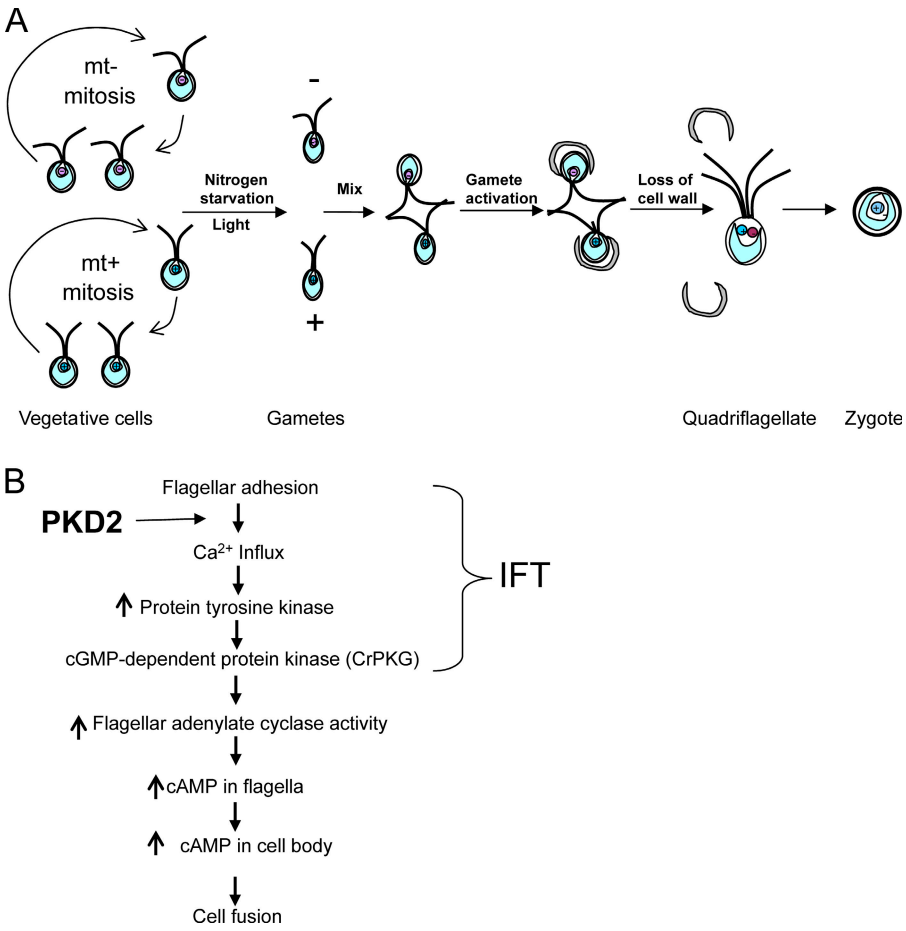


Figure 8. **Diagram of the mating process in *C. reinhardtii*.** (A) When starved for nitrogen in the light, mt+ and − vegetative cells differentiate into gametes. When mixed, the gametes adhere by their flagella and become activated, resulting in the loss of their cell wall, assembly of mating structures (visible in mt+ gametes), and cell fusion to form a dikaryon. The two nuclei fuse in the dikaryon, producing the diploid zygote. (B) Flagellar adhesion initiates a signal cascade involving a calcium influx and an increase in cAMP in the cell body. IFT is important for the first steps of this pathway after flagellar adhesion.

levels (Fig. 9 B). Mating efficiency was measured as the percentage of gametes fused to form quadriflagellates after mixing mt+ gametes of wild-type or CrPKD2-depleted strains with mt− wild-type gametes (see Materials and methods). Compared with wild-type gametes, the RNAi cells showed up to a 75% reduction in mating efficiency, and the severity of the defect correlated with the extent of CrPKD2 depletion (Fig. 9, B and C).

Inefficient mating could be caused by a failure of cells to form gametes when starved for nitrogen. To determine whether CrPKD2-depleted cells expressed agglutinins on their flagellar surface during gametogenesis, aggregation of mt+ and − gametes was observed. RNAi knockdown gametes appeared to adhere normally to wild-type gametes of the complementary mt, demonstrating that there was no obvious defect in gametogenesis and that the flagellar agglutinins were expressed normally on the flagella of the CrPKD2-depleted gametes. For a more complete assessment of the ability of the CrPKD2-depleted gametes to mate, mating was done in the presence of cAMP. The addition of cAMP to the mating reaction bypasses the initial stages of the signaling pathway where a calcium influx is required (Fig. 8 B; Goodenough, 1989). The mating efficiency was restored in CrPKD2-depleted gametes by the addition of 15 mM dibutyryl-cAMP and 0.15 mM papaverine, indicating that these gametes were competent to mate. To investigate the effect of CrPKD2 depletion on signaling events upstream of the increase in cAMP, the phosphorylation state of a CrPKG, a protein known to be phosphorylated after flagellar adhesion in wild-type cells (Wang and Snell, 2003; Wang et al., 2006), was assayed. Phosphorylation of CrPKG was reduced in matings of the RNAi46 strain to the wild type (Fig. 9 D), suggesting that CrPKD2 functions in mating between flagellar adhesion and CrPKG phosphorylation. The residual phosphorylation of CrPKG in these matings was caused by its phosphorylation in the wild-type gametes used to mate with the CrPKD2-depleted gametes.

## Discussion

In this study, the *C. reinhardtii* homologue of a PKD2 family member was cloned. CrPKD2 was found to have the hallmarks of vertebrate polycystin-2, a cation channel located on primary cilia (Pazour et al., 2002; Yoder et al., 2002). We have exploited various advantages of this organism to investigate the flagellar form of CrPKD2 and examine its signaling function. This work shows that CrPKD2 is cleaved in the cell body, that the cleavage products can be found in isolated, purified flagellar membranes, that some of the CrPKD2 is immobilized, possibly by linkage to the flagellar axoneme, and that a small portion of the total CrPKD2 in the flagella moves in an IFT-dependent manner. By use of RNAi CrPKD2 knockdowns, we have also shown that the CrPKD2 channel plays a role in the initial steps of the well-characterized signaling cascade that occurs in the flagella during mating.

### Flagellar CrPKD2 is cleaved

Analysis of the *C. reinhardtii* flagellar proteome indicated that a PKD2 family homologue was present in *C. reinhardtii* flagella (Pazour et al., 2005). Cloning and sequencing this gene indicated that this protein has the hallmarks of PKD2, including the six transmembrane domains showing homology to cation channels. Immunoblots of purified flagella confirmed that the protein is present in flagella. Interestingly, the full-length (210-kD) form of CrPKD2 was not present in the flagella; rather, two smaller forms (120 and 90 kD) were present. This is the first study showing cleavage of a PKD2 family member. These fragments can be generated in the cell body by cleavage of full-length CrPKD2. Although it seems likely that the CrPKD2 fragments move into the flagella after cleavage, we cannot rule out the possibility that full-length CrPKD2 moves into the flagella and is rapidly cleaved.

Like CrPKD2, other ciliary membrane proteins involved in PKD are known to undergo cleavage. For example, the long extracellular N terminus of PKD1 is cut near the first transmembrane domain and reattached to the C-terminal fragment (Qian et al., 2002). Likewise, fibrocystin undergoes several proteolytic cleavages, resulting in an extracellular fragment that is shed from the primary cilium (Kaimori et al., 2007). Proteolysis is also involved in the maturation of channels such as the heterotrimeric epithelial $Na^+$ channel, in which the cleavage of the extracellular loops occurs at two sites within the α subunit and at a single site within the γ subunit (Carattino et al., 2006). The inositol 1,4,5-trisphosphate receptor is cleaved by caspase 3, removing a regulatory element from the channel, and thereby allowing a rapid increase in cytosolic $Ca^{2+}$ during apoptosis (Assefa et al., 2004; Nakayama et al., 2004). One member of the TRP family of channels belonging to the TRPML class is also known to undergo cleavage (Kiselyov et al., 2005; Miedel et al., 2006). This class, like CrPKD2, is characterized by a large extracellular loop, and in both cases proteolysis occurs in this loop. Thus, cleavage is emerging as a mechanism for regulation of channel activity and may be a general feature of TRP channels with large extracellular loops, including members of the TRPP2 family.

To further study flagellar CrPKD2, we optimized methods for isolating flagellar membranes using nonionic detergent, either with or without freeze–thaw treatment, to remove the membranes from isolated flagella followed by purification of the released membranes on Optiprep density gradients. The resultant membranes had little axonemal contamination as determined by thin section EM and immunoblots of the membrane fractions with axonemal antibodies and contained most of the flagellar CrPKD2. The remainder of the CrPKD2 appeared to be bound to the axoneme, and the two CrPKD2 fragments partitioned together in both the membrane and axonemal fractions. Cofractionation leaves open the possibility that the two fragments interact with each other, as is the case with TRPML-1 (Kiselyov et al., 2005), but such an interaction has not yet been demonstrated. Although we do not know the significance of the apparent attachment of CrPKD2 to the axoneme, it may be instrumental in CrPKD2 function. Interactions of kinesin-2 and tubulin with PKD2 have been shown to affect PKD2 activity in vitro (Wu et al., 2006; Montalbetti et al., 2007).

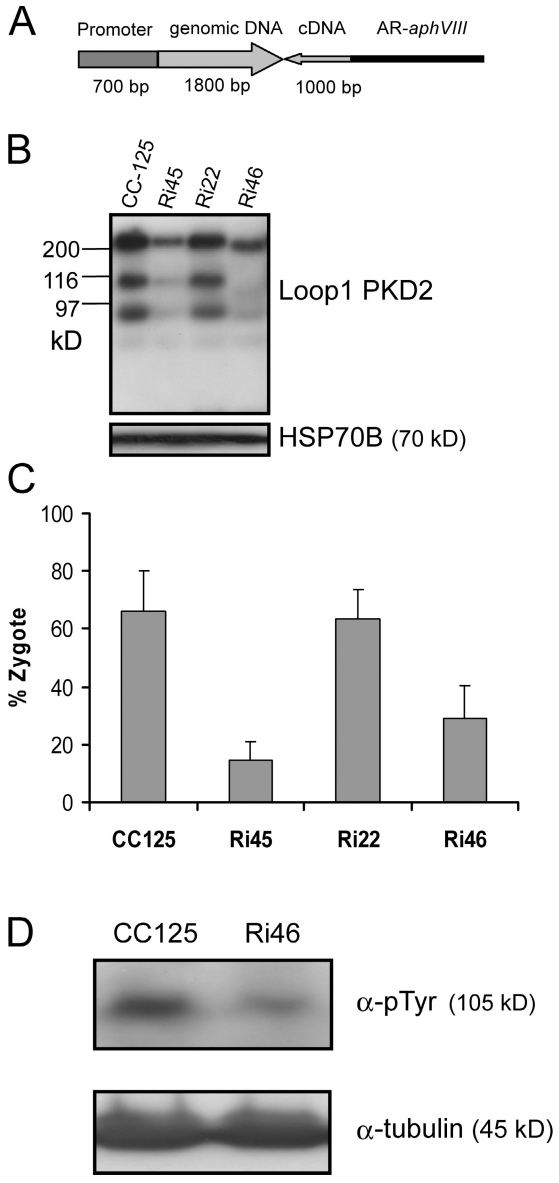


Figure 9. **CrPKD2 is involved in mating.** (A) The construct used for RNAi included 1,000 bp of the *CrPKD2* cDNA (5′ UTR and first two exons) appended antisense to the corresponding genomic fragment, driven by the native promoter. *AphVIII* is a selectable marker gene driven by the *HSP70A-RbcS2* fusion promoter (Sizova et al., 2001). (B) Immunoblot analysis shows a reduced amount of CrPKD2 in RNAi transformants Ri45 and Ri46 compared with wild-type cells. An HSP70B antibody was used as a loading control (Schroda et al., 1999). (C) Histogram showing the decrease in mating efficiency that occurs in RNAi transformants with reduced levels of CrPKD2. Bars represent the mean ± SEM from three independent experiments. (D) Protein tyrosine kinase activity was assayed in vitro in flagellar proteins isolated from mated gametes. Samples were incubated for 30 min and analyzed on immunoblots probed with antibodies against the phosphotyrosine residue of CrPKG (α-pTyr) or α-tubulin as loading control. Phosphorylation of CrPKG is reduced in flagellar extracts of gametes of the RNAi46 strain.

### Movement of flagellar CrPKD2

IFT moves axonemal precursor polypetides to the flagellar tip for assembly (Qin et al., 2004; Hou et al., 2007) and it also moves the TRPV channels OSM-9 and OCR-2 within the plane of the membrane of *C. elegans* sensory cilia (Qin et al., 2005). However, in these sensory cilia, PKD2 did not appear to move

(Qin et al., 2005). In this paper, we show that though >90% of the flagellar CrPKD2 remains stationary, occasionally puncta of CrPKD2 moved to the flagellar tip at a rate similar to that of IFT. Similar movement of a small portion of the *C. elegans* sensory cilia PKD2 might not have been detected because of the difficulty in imaging these short, interstitial cilia. The movement of *C. reinhardtii* flagellar PKD2 was confirmed by photobleaching studies in which a 19% recovery of CrPKD2–GFP fluorescence was observed 2 min after bleaching. Blocking IFT in *fla10* cells at restrictive temperature reduced this recovery by 50%, further substantiating the role of IFT in CrPKD2 dynamics in the membrane.

Another manifestation of the participation of IFT in moving CrPKD2 was seen by inactivating the IFT anterograde motor kinesin-2 in the temperature-sensitive mutant *fla10,* which resulted in a paradoxical accumulation of CrPKD2 in the flagella. Similar accumulations of CrPKD2 occur as a result of perturbation of IFT in sensory cilia of *C. elegans* (Qin et al., 2001) and primary cilia in murine kidneys (Pazour et al., 2002). The accumulation of PKD2 in the cilia of all three organisms might be explained if a mechanism other than IFT can move PKD2 into the cilium, but retrograde IFT is necessary to move PKD2 out. Indeed, KLP-6 is required to move PKD2 into cilia of *C. elegans* (Peden and Barr, 2005), and KIF17, an OSM-3 homologue that is also found in the *C. reinhardtii* genome, transports cyclic nucleotide-gated channels to the cilia in murine cells (Jenkins et al., 2006). Support for a mechanism other than kinesin-2 in the movement of CrPKD2 in *C. reinhardtii* flagella comes from our observation that some recovery of fluorescence follows photobleaching in the absence of IFT (i.e., *fla10* at nonpermissive temperature). CrPKD2 moved into the flagellum by a mechanism other than IFT would accumulate there in the absence of removal by retrograde IFT, which is also defective in *fla10* at restrictive temperature (presumably because the retrograde motor is no longer being carried to the distal tip of the flagellum; Cole et al., 1998; Iomini et al., 2001). Although no retrograde movement of CrPKD2–GFP was detected, such movement may occur beneath our level of detection.

### CrPKD2 is involved in the mating signal pathway

PKD2 plays a role in the mating of several organisms as well as *C. reinhardtii*: the acrosomal reaction triggered when sea urchin sperm bind egg jelly requires PKD1 and 2 (Neill et al., 2004); the proper entrance of sperm into the sperm storage organ of female *D. melanogaster* is dependent on PKD2 (Gao et al., 2003; Watnick et al., 2003); and LOV1 (a PKD1 homologue) and PKD2 are required on sensory cilia of *C. elegans* for location of the vulva by male nematodes (Barr and Sternberg, 1999). The mating of *C. reinhardtii* is a process that is initiated when the flagella of gametes of opposite mt adhere to one another via interactions of mt-specific agglutinins on the surface of flagella. This triggers a signaling cascade that ultimately results in the fusion of the gametes to form a zygote. Several components of this pathway are known (Fig. 8 B), and pharmacological experiments implicate calcium as a key player in the initial stages of this process.

One of the early stages of the signaling pathway, phosphorylation of CrPKG, does not occur after inactivation of IFT (Wang and Snell, 2003; Wang et al., 2006) or depletion of CrPKD2 (this paper). When gametes of the temperature-sensitive kinesin-2 mutant *fla10* are incubated at 32°C before mixing with gametes of the opposite mt, flagellar adhesion occurs, but the activation of CrPKG is abolished (Pan and Snell, 2002; Wang and Snell, 2003; Wang et al., 2006) and the cells are unable to fuse. Likewise, in this study, CrPKG was not activated in CrPKD2-depleted gametes even though their flagella adhered to those of gametes of the opposite mt. Given that PKD2 can act as a mechanosensitive cation channel, it is reasonable to speculate that agglutinin binding and flagellar adhesion serve as the stimuli that cause CrPKD2 to admit a $Ca^{2+}$ influx into the flagellar compartment and initiate the signaling pathway. Because there is no clear homologue of PKD1 in the *C. reinhardtii* genome, it may be that agglutinins assume the role of regulating the channel activity of CrPKD2 during the mating of *C. reinhardtii*.

Several issues about ciliary signaling are highlighted by this work on flagellar PKD2. First, is cleavage of ciliary PKD2 a widespread phenomenon, and what is its role in the function of the protein? Second, how is the signal that is initiated by increased $Ca^{2+}$ in the cilium transmitted to the cell body? It is doubtful that this occurs by calcium diffusion because free calcium ions are generally unable to diffuse more than 0.5 μm in the cell given the typical concentration of calcium-binding proteins (Clapham, 1995). Propagation of the signal to the cell body may require secondary messengers, like cAMP, which is known to become elevated in the flagella of *C. reinhardtii* during the mating reaction. Third, what are the roles of IFT in signal transduction pathways in cilia? IFT is known to be essential for the formation of this sensory organelle and also appears to regulate the concentration of sensory molecules, like PKD2, in cilia (Follit et al., 2006). In addition, IFT may be directly involved in the completion of signaling pathways by transporting the signal itself, possibly in the form of a posttranslationally modified protein (Chauvet et al., 2004; Low et al., 2006). Thus, it will be of great interest to elucidate further details of the ciliary PKD2 signaling pathway and its relationship to other PKD-related proteins and to develop *C. reinhardtii* as an in vivo assay for screening compounds for therapeutic activity in treating PKD.

The first clues that cilia were involved in the pathogenesis of PKD came from the characterization of the IFT-dependent flagellar assembly process in *C. reinhardtii* (Pazour et al., 2000). The presence of CrPKD2 along with homologues of many PKD-related proteins in the flagella of *C. reinhardtii* demonstrates that this organism will continue to act as an attractive model for the study of the cilium as a sensory antenna and of its involvement in a wide spectrum of cilia-related diseases (Pan et al., 2005; Pazour et al., 2005).

## Materials and methods

#### Cell and culture media

The *C. reinhardtii* wild-type strains CC-125 (mt+) and CC-124 (mt−), paralyzed flagella strain *pf18* (CC-1297, mt−), temperature-sensitive flagellar assembly mutant *fla10* (*fla10-1* allele, CC-1919, mt−), and *arg*⁻ strain CC-3681 (*arg7*, mt−) were obtained from the Chlamydomonas Genetics Center.

The *arg2 pf1* double mutant was generated by K. Kozminski (University of Virginia, Charlottesville, VA). Cells were grown on solid media supplemented with 1.5% agar or in a liquid minimal medium, MI (Harris, 1989), MI-N (MI medium without nitrogen to induce gametogenesis), or Tris-acetate-phosphate media (Harris, 1989) at 22–23°C with a 14/10-h light/dark cycle and constant aeration.

**Cloning of the *CrPKD2* gene**

The EST clone AV395567 (Asamizu et al., 1999) corresponding to the predicted CrPKD2 protein C_590099 (Joint Genome Institute version 2 draft assembly of the *C. reinhardtii* genome) was sequenced. It included the sequence from bp 1,223 of the cDNA through the 3′ UTR of *CrPKD2*. We extended the cDNA to the 5′ UTR by sequencing the two RT-PCR products generated using two sets of primers: TCTTGGGAGTGCTGTATGAGCAGCGC (bp 318–343 of the cDNA) and CGGTGGTGTTGTACACGATGC (bp 1,696–1,716 of the cDNA); and AAGTAGCATGTCACATTAATGCATG (bp 1–25 of the cDNA) and CCGACACCGACTGGTTAAGGT (bp 1,125–1,145 of the cDNA), which were generated according to the *C. reinhardtii* genome sequence database (http://genome.jgi-psf.org/chlre2/chlre2.home.html). The mRNA was isolated and reverse transcribed as described previously (Huang et al., 2002). The RT-PCR products were cloned into PCRII-TOPO (Invitrogen), generating plasmids pHK5 and pHK15, respectively. The intron coded by genomic DNA was not present in the PCR products.

**Antibody production**

Loop1 CrPKD2 antibodies were generated against a His-tagged fragment of CrPKD2 (aa 358–1,019) expressed in *E. coli* and purified by affinity chromatography using nickel–nitrilotriacetic acid agarose according to the manufacturer's instructions (QIAGEN). The purified protein was used for antibody production in rabbits at Pocono Rabbit Farm and Laboratory Inc. A peptide (AGEGDDKDDSPEVREEKRK, corresponding to aa 1,444–1,462 of CrPKD2) was synthesized and used to produce a second antibody by the same company. The N-PKD2 antibody was affinity purified from the Loop1 antiserum using a peptide containing aa 358–583 of CrPKD2, which was expressed in *E. coli* and purified using nickel–nitrilotriacetic acid agarose.

**Flagellar isolation and flagellar membrane vesicle isolation**

Flagella were isolated from *C. reinhardtii* by pH shock as described previously (Witman et al., 1972) and modified by Cole et al. (1998). The flagella from 40–48 liters of wild-type cells were resuspended in 6 ml HMDEK buffer (10 mM Hepes, pH 7.2, 5 mM $MgSO_4$, 1 mM DTT, 0.5 mM EDTA, and 25 mM KCl, including the protease inhibitors 1.0 mM PMSF, 50 μg/ml soybean trypsin inhibitor, 1 μg/ml pepstatin A, 2 μg/ml aprotinin, and 1 μg/ml leupeptin) for a protein concentration of ~3–4 μg/μl, and NP-40 (Calbiochem) was added to a final concentration of 0.1%. The mixture was incubated at 4°C for 30 min with shaking. The membrane vesicles were separated from the axonemes by centrifugation at 16,000 *g* for 10 min at 4°C, the supernatant was centrifuged again to remove any remaining axonemes, and the membranes were harvested by centrifugation at 228,000 *g* for 30 min (TLA 120.2 rotor, Optima Ultracentrifuge; Beckman Coulter). The pellet was resuspended in 1 ml of 0.1% NP-40 HMDEK buffer and centrifuged again to obtain the final pellet. Alternatively, membranes were further purified by density gradient sedimentation. For this, 1/3 volume of 60% iodixanol (Optiprep density gradient medium; Sigma-Aldrich) was added to the membrane-containing supernatant for a final concentration of 15%, and 0.9 ml of the mixture was added to a 1.5-ml tube. After underlaying with 0.3 ml of 30% iodixanol in HMDEK + 0.1% NP-40 buffer, the sample was centrifuged for 1 h and 11 min at 431,000 *g*. A white band of membrane vesicles in the middle of the tube was collected and diluted 10 times with 0.1% NP-40 HMDEK buffer. The mixture was split and centrifuged as before, sedimenting the membrane vesicles. One membrane pellet was used for EM and the other was resuspended in 100–200 μl HMDEK buffer with 0.1% NP-40 for immunoblotting.

To remove all the flagellar membrane from the axoneme, the flagella were freeze–thawed twice to release the matrix and a small amount of membrane. Much of the membrane remained in the axonemal pellet. The axonemes were exacted twice with 0.1 or 1% NP-40 at room temperature for 30 min, and after centrifugation at 16,000 *g* for 10 min, the soluble fractions contained the membrane and the pellet contained axonemes. The membranes were sedimented at 280,000 *g* for 30 min.

**Protein extraction, concentration determination, and immunoblot analysis**

Preparation of the *C. reinhardtii* whole cell extract, determination of the protein concentration, PAGE, and immunoblotting were performed as described previously (Huang et al., 2002). Immunoblots were scanned and the relative protein concentrations were determined using ImageJ (National Institutes of Health).

**GFP constructs and transformation with CrPKD2–GFP**

To make the CrPKD2–GFP fusion, the *C. reinhardtii* bacterial artificial chromosome clone 18K16 (https://www.genome.clemson.edu/cgi-bin/orders) was cut with EcoRV and SpeI, generating an ~18-kb fragment, which included the entire *CrPKD2* gene and its promoter. This fragment was subcloned into the EcoRV and SpeI sites of pBluescript II KS+ (Stratagene), generating a plasmid named pHK25. This plasmid was cut with HindIII, generating three fragments. One of these fragments, an 8-kb fragment containing the promoter and most of the genomic DNA encoding CrPKD2, was cloned into the HindIII site of the pBluescript KS+, generating pHK28. A second fragment, a 5.8-kb fragment containing the last two introns, exons, the 3′ UTR of *CrPKD2*, and the KS+ vector, was religated to produce pHK26.

To tag the *CrPKD2* gene, we cloned the *GFP* gene into a unique EcoRI site in intron 11, flanked by the first intron of RBCS2 (Goldschmidt-Clermont and Rahire, 1986). For this, the two ends of the intron were subcloned as follows: using the genomic DNA as template, the 3′ end of this intron was amplified with the primers CG**GAATTC**AGTCGACGAGCAAGCC and GT**GGATCC**TCCTGCAAATGGAAAC. EcoRI and BamHI sites (added sites in bold) were added to the primers and the PCR product was cut with EcoRI and BamHI and cloned into the same sites of pBluescript II KS+ vector (pHK31). Another set of primers was used to amplify the 5′ end of the first intron of the RBCS2: CA**GGATCC**CCAGGTGAGTTCGACGAGCAAG including a BamHI site and C**TCTAGAGAATTC**AAATGGAAACGGCGACG including XbaI and EcoRI sites. The PCR product was cut with BamHI and XbaI and cloned into pHK31 (BamHI and XbaI sites), generating pHK32. The BamHI fragment of the pCrGFP (Entelechon GmbH), which contains the *C. reinhardtii* codon-adapted GFP ending with a stop codon, was inserted into the BamHI site of pHK32, generating pHK35. The sense orientation of this and following inserts was identified by restriction enzyme digests and confirmed by sequencing. The EcoRI fragment from pHK35 was inserted into the EcoRI site in intron 11 of the *CrPKD2* gene of pHK26 in the sense orientation, generating pHK37. The 8-kb HindIII fragment that contains the promoter and 5′ end of *CrPKD2* was inserted in the HindIII site of pHK37 in the sense orientation, generating pHK38.

To remove the stop codon at the end of *GFP* from pHK38, two primers, AGGTCGACTCTAGA**GGATCC**C and T**GGATCC**TTGTACAGCTCGTCCATGCCG, both containing a BamHI site, were used to amplify the *GFP* fragment. The PCR product, which did not have the *GFP* stop codon, was cloned into the TOPOII-PCR vector (Invitrogen), generating plasmid pHK34. The BamHI fragment of the pHK34 was exchanged with the BamHI fragment of pHK37 (which has a stop codon at the end of the *GFP* gene), generating plasmid pHK39. The HindIII fragment of pHK28 was inserted into pHK39 in the sense orientation to generate pHK41. Plasmids pHK38 and pHK41 were linearized with SpeI before transformation.

Because we did not observe fluorescence in transformants that harbor pHK38 or 41, these cells were only used for immunoblots, and the overlap PCR method was used to make another construct in which GFP was fused to the end of CrPKD2 through a flexible linker. Using the left (GGAGA**AAGCTT**GTGTTTTGG, HindIII) and right primers (CGCGCCGGAGGCGCCCTGGCCGGAGGCGCCCTGGGGCGGGGTCTCATTCATCA) and pHK26 as the template to amplify the C terminus of CrPKD2, the PCR product containing the fragment from the HindIII site in the last intron to the stop codon of CrPKD2 was obtained. The nucleotide sequence GGCGCCTCCGGCCAGGGCGCCTCCGGCGCG, which corresponds to a flexible protein linker GASGQGASGA, was included in the right primer. Another set of primers (GGCGCCTCCGGCCAGGGCGCCTCCGGCGCGAAGGGCGAGGAGCTGTTCACC and CTC**GGTACC**CGCTTCAATACG, KpnI) was used to amplify *GFP* and the 3′ UTR of RBCS2 from the plasmid pCrGFP. The sequence encoding the protein linker was included in the left primer. Both PCR products were purified using a PCR purification kit (QIAGEN), and equal molar amounts of the products were used as templates to fuse these two PCR products together. For this purpose, primers (GGAGA**AAGCTT**GTGTTTTGG [HindIII] and CTC**GGTACC**CGCTTCAATACG [KpnI]) were used, and the new PCR product was cut with HindIII and KpnI and cloned into the pBluescript II KS+ vector (HindIII and KpnI sites). The resulting plasmid was named pHK49. The HindIII fragment from pHK28 was inserted into the HindIII site of pHK49 in the sense orientation, generating pHK52. pHK52 was linearized with SpeI before transformation.

To prepare cells (CC-3681, *arg7*, and *arg2 pf1)* for transformation, cell walls were removed with autolysin as described previously (Huang and Beck, 2003). Linearized plasmids pHK38, pHK41, and pHK52, together

with pCB412, which harbors an *AGR7* gene as a selectable marker (gift from C.F. Beck, University of Freiburg, Freiburg, Germany), were introduced into the cells using the glass bead method. Transformants were selected on Tris-acetate-phosphate medium plates and tested for GFP by Western blot analysis. GFP antibody was obtained from Roche Applied Science (clones 7.1 and 13.1).

To construct the *fla10* (mt−) and *pf18* (mt−) strains expressing CrPKD2–GFP, the original *CrPKD2–GFP* transformant (mt−) was crossed to CC-125 (mt+) to produce an mt+ strain. This strain was crossed with *fla10* and *pf18*, and the progeny were analyzed to obtain the desired phenotype.

### Nucleic acid manipulations and transformation of CrPKD2 interference construct

To make the genomic and cDNA fusion construct for RNAi, primers (GGACATGGTTCGTAGCGTTTAATGCC [700 bp in front of the translation start site of *CrPKD2* gene] and **GTCGAC**CGACACCGACTGGTTAAGGT [corresponding to the cDNA 1,145–1,125]), including a SalI site, were used to amplify the promoter and 5′ region of the *CrPKD2* gene using genomic DNA as a template. The 2.5-kb PCR product was cloned into TOPO TA vector with the 3′ SalI site near the EcoRV site of the vector, generating plasmid pHK3. Another set of primers (AAGTAGCATGTCACATTAATGCATG [corresponding to bp 1–25 of the cDNA] and **GTCGAC**CGACACCGACTGGTTAAGGT [corresponding to the cDNA 1,145–1,125]), including a SalI site, were used to amplify the *PKD2* cDNA fragment, which corresponds to the genomic fragment in pHK3. The PCR product was cloned into the TOPO TA vector, and a clone with the 5′ end near the EcoRV site was identified and named pHK15. The EcoRV and SalI fragment from the plasmid pHK15 was inserted into the same sites in pHK3, creating pHK19. The PvuII fragment of pSI103 (Sizova et al., 2001), which includes the aphVIII gene driven by the HSP70A-RBCS2 fusion promoter, was inserted into the EcoRV site of the pHK19, generating pHK22 (Fig. 7 A). pHK22 was linearized with ScaI before transformation using the glass bead method. Transformants were selected on plates with 10 μg/ml paromomycin (Sigma-Aldrich) and tested for PKD2 levels by Western blot analysis. 95 transformants were screened and 15 clones were picked for further analysis. Eventually, four clones showed a stable reduction of CrPKD2. Two of these (Ri22 and Ri39) showed only a modest decrease, and only one of these is included. The other two (Ri45 and Ri46) showed a more substantial depletion of CrPKD2.

### Immunofluorescence light microscopy, live cell imaging, and FRAP

Wild-type strains were prepared for immunofluorescence light microscopy using methanol fixation, and were stained with primary and Alexa fluor–conjugated secondary antibodies (Invitrogen) as described previously (Pedersen et al., 2003), modified by the addition of 0.05% glutaraldehyde directly to the medium for primary fixation before fixing with methanol at −20°C. Images were recorded with a microscope (Eclipse TE2000; Nikon) equipped with a Plan Apo 100×, 1.4 NA objective lens and a forced-air–cooled camera (Cascade 512B; Photometrics). Photoshop (Adobe) was used to adjust brightness and contrast and crop images.

The movement of the GFP-tagged CrPKD2 was recorded as described in the previous paragraph using an argon ion 488 laser controlled by a Mosaic System (Photonics) for illumination and photobleaching experiments.

For photobleaching, *fla10* cells were immobilized with 0.02-M LiCl (Dentler, 2005) and embedded in 0.75% low-melt agarose. First, a DIC picture was taken of the flagellum, and the GFP fluorescence of the selected region was recorded for 2 s using laser illumination at 32 mW ($F_{prebleach}$). Next, the selected region of the flagellum was bleached for 3 s with the laser at 300 mW. GFP fluorescence of the selected region was recorded again for 2 s using the laser at 32 mW ($F_{bleached}$). After 1 or 2 min of recovery, the GFP fluorescence of the selected region was recorded for 2 s at low power ($F_{recovery}$). Finally, another DIC picture of the flagellum was taken. By comparing the two DIC pictures of the same flagellum, videos were selected for further analysis in which the flagellum did not move and the focus did not change. The mean fluorescence of each parameter, $F_{prebleach}$, $F_{bleached}$, and $F_{recovery}$, were used to calculate recovery: % recovery = $(F_{recovery} - F_{bleached})/F_{prebleach}$. For performing the experiment at 32°C, cells were incubated at 32°C in a water bath and observed for a maximum of 10 min at room temperature on the microscope. Alternatively, cells were observed in a glass-bottom Petri dish (WillCo Wells B.V.) in a stage-mounted dish heater (DH-35; Warner Instruments). Data were analyzed using MetaMorph (Universal Imaging Corp).

### Flagellar length measurements

*fla10* cells were maintained at 22 or 32°C to induce flagellar resorption. Wild-type cells were induced to resorb their flagella with 20 mM NaPPi. Aliquots of these cells were fixed with 1% glutaraldehyde. Cells were imaged as described in the previous section and the lengths of individual flagella were measured using the MetaMorph software package.

### Measurement of mating efficiency and flagellar protein tyrosine kinase activity

Gametes were generated by resuspending vegetative cells in MI-N medium at a density of 1–2 × $10^7$ cells/ml. The cells were incubated under continuous light for 16–24 h and gametes (CC-125 and RNAi strains) were adjusted to the same cell density. The gametes to be assayed were mixed with a twofold excess of gametes of the opposite mt (CC-124) to ensure that mating efficiency of the test strains was not limited by depletion of the mating partner. After completion of the mating reaction in 1 h, the cells were fixed by addition of glutaraldehyde, and the number of the quadriflagellate zygotes and biflagellate cells were counted by phase-contrast microscopy (Martin and Goodenough, 1975; Beck and Acker, 1992). The percentage of cells that had mated was then calculated according to the method of Beck and Acker (1992).

To assay flagellar protein tyrosine kinase activity, gametes of CC-125 or Ri46 were mixed with the same number of CC-124 gametes, and flagella were isolated 3 min after mixing. The concentration of the flagellar protein was measured using the Amido black method (Huang et al., 2002), and equivalent amounts of protein were used to assay the protein tyrosine kinase activity by immunoblotting for phosphorylated CrPKG, the substrate of protein tyrosine kinase (Wang and Snell, 2003).

### EM

Axonemes and membrane pellets were treated sequentially at room temperature for 1 h each with 2.5% glutaraldehyde in HMDEK, 1% osmium tetroxide in HMDEK, and 1% uranyl acetate in water with brief rinses in between. The pellets were dehydrated through ethanol and propylene oxide and embedded in epoxy resin according to standard procedures. The final steps of dehydration and the initial steps of resin infiltration were performed at −20°C for the membrane samples. Silver sections were observed with an electron microscope (1230; JEOL) equipped with a digital camera (Orca HR; Hamamatsu Photonics).

### RNA isolation and Northern blot hybridization

Gametes were deflagellated using the pH shock method and vigorously aerated under light. Total RNA was isolated from cells before deflagellation and after 10 or 15 min of flagellar regeneration. RNA was blotted and hybridization was performed as described previously (von Gromoff et al., 1989).

### Online supplemental material

Table S1 lists the lengths of flagella measured from cells induced to resorb their flagella. Fig. S1 shows a diagram of the *CrPKD2* gene and the amino acid sequence of the protein. Fig. S2 shows a phylogenetic tree of TRP channels. The Northern blots in Fig. S3 demonstrate that only one 6-kbp transcript is present encoding CrPKD2. Additional immunoblots of the CrPKD2 fragments from cells expressing CrPKD2–GFP are shown in Fig. S4. Video 1 shows the movement of CrPKD2 in the flagella of *fla10* gametes at permissive temperature. The online version of this article is available at http://www.jcb.org/cgi/content/full/jcb.200704069/DC1.

We thank Hue Tran for preparation of *C. reinhardtii* flagella and Roshan Karki for EM. We are grateful to Professor C.F. Beck for the pCB412 plasmid and to Professor M. Hippler for micropeptide sequencing.

This work was supported by grants from the National Institutes of Health (GM014642 to J.L. Rosenbaum, GM30626 to G.B. Witman, and GM060992 to G.J. Pazour) and a grant from the Polycystic Disease Foundation (159a2f) to K. Huang. G.B. Witman also received funding from the Robert W. Booth Fund at the Greater Worcester Community Foundation.

Submitted: 13 April 2007
Accepted: 10 October 2007

## References

Asamizu, E., Y. Nakamura, S. Sato, H. Fukuzawa, and S. Tabata. 1999. A large scale structural analysis of cDNAs in a unicellular green alga, *Chlamydomonas reinhardtii*. I. Generation of 3433 non-redundant expressed sequence tags. *DNA Res.* 6:369–373.

Assefa, Z., G. Bultynck, K. Szlufcik, N. Nadif Kasri, E. Vermassen, J. Goris, L. Missiaen, G. Callewaert, J.B. Parys, and H. De Smedt. 2004. Caspase-3-induced truncation of type 1 inositol trisphosphate receptor accelerates

apoptotic cell death and induces inositol trisphosphate-independent calcium release during apoptosis. *J. Biol. Chem.* 279:43227–43236.

Avidor-Reiss, T., A.M. Maer, E. Koundakjian, A. Polyanovsky, T. Keil, S. Subramaniam, and C.S. Zuker. 2004. Decoding cilia function: defining specialized genes required for compartmentalized cilia biogenesis. *Cell*. 117:527–539.

Barr, M.M., and P.W. Sternberg. 1999. A polycystic kidney-disease gene homologue required for male mating behaviour in *C. elegans. Nature*. 401:386–389.

Beck, C.F., and A. Acker. 1992. Gametic differentiation of *Chlamydomonas reinhardtii*: Control by nitrogen and light. *Plant Physiol.* 98:822–826.

Bergman, K., U.W. Goodenough, D.A. Goodenough, J. Jawitz, and H. Martin. 1975. Gametic differentiation in *Chlamydomonas reinhardtii*. II. Flagellar membranes and the agglutination reaction. *J. Cell Biol.* 67:606–622.

Bloodgood, R.A., and E.N. Levin. 1983. Transient increase in calcium efflux accompanies fertilization in *Chlamydomonas. J. Cell Biol.* 97:397–404.

Bloodgood, R.A., M.P. Woodward, and N.L. Salomonsky. 1986. Redistribution and shedding of flagellar membrane glycoproteins visualized using an anti-carbohydrate monoclonal antibody and concanavalin A. *J. Cell Biol.* 102:1797–1812.

Brazelton, W.J., C.D. Amundsen, C.D. Silflow, and P.A. Lefebvre. 2001. The *bld1* mutation identifies the *Chlamydomonas osm-6* homolog as a gene required for flagellar assembly. *Curr. Biol.* 11:1591–1594.

Carattino, M.D., S. Sheng, J.B. Bruns, J.M. Pilewski, R.P. Hughey, and T.R. Kleyman. 2006. The epithelial Na+ channel is inhibited by a peptide derived from proteolytic processing of its alpha subunit. *J. Biol. Chem.* 281:18901–18907.

Chauvet, V., X. Tian, H. Husson, D.H. Grimm, T. Wang, T. Hiesberger, P. Igarashi, A.M. Bennett, O. Ibraghimov-Beskrovnaya, S. Somlo, and M.J. Caplan. 2004. Mechanical stimuli induce cleavage and nuclear translocation of the polycystin-1 C terminus. *J. Clin. Invest.* 114:1433–1443.

Clapham, D.E. 1995. Calcium signaling. *Cell*. 80:259–268.

Cole, D.G. 2003. The intraflagellar transport machinery of *Chlamydomonas reinhardtii. Traffic*. 4:435–442.

Cole, D.G., D.R. Diener, A.L. Himelblau, P.L. Beech, J.C. Fuster, and J.L. Rosenbaum. 1998. *Chlamydomonas* kinesin-II-dependent intraflagellar transport (IFT): IFT particles contain proteins required for ciliary assembly in *Caenorhabditis elegans* sensory neurons. *J. Cell Biol.* 141:993–1008.

Davenport, J.R., and B.K. Yoder. 2005. An incredible decade for the primary cilium: a look at a once-forgotten organelle. *Am. J. Physiol. Renal Physiol.* 289:F1159–F1169.

Deane, J.A., D.G. Cole, E.S. Seeley, D.R. Diener, and J.L. Rosenbaum. 2001. Localization of intraflagellar transport protein IFT52 identifies basal body transitional fibers as the docking site for IFT particles. *Curr. Biol.* 11:1586–1590.

Dentler, W. 2005. Intraflagellar transport (IFT) during assembly and disassembly of *Chlamydomonas* flagella. *J. Cell Biol.* 170:649–659.

Dutcher, S.K., N.S. Morrissette, A.M. Preble, C. Rackley, and J. Stanga. 2002. Epsilon-tubulin is an essential component of the centriole. *Mol. Biol. Cell*. 13:3859–3869.

Follit, J.A., R.A. Tuft, K.E. Fogarty, and G.J. Pazour. 2006. The intraflagellar transport protein IFT20 is associated with the Golgi complex and is required for cilia assembly. *Mol. Biol. Cell*. 17:3781–3792.

Fuhrmann, M., A. Stahlberg, E. Govorunova, S. Rank, and P. Hegemann. 2001. The abundant retinal protein of the *Chlamydomonas* eye is not the photoreceptor for phototaxis and photophobic responses. *J. Cell Sci.* 114:3857–3863.

Gabow, P.A. 1993. Autosomal dominant polycystic kidney disease. *N. Engl. J. Med.* 329:332–342.

Gao, Z., D.M. Ruden, and X. Lu. 2003. PKD2 cation channel is required for directional sperm movement and male fertility. *Curr. Biol.* 13:2175–2178.

Goldschmidt-Clermont, M., and M. Rahire. 1986. Sequence, evolution and differential expression of the two genes encoding variant small subunits of ribulose bisphosphate carboxylase/oxygenase in *Chlamydomonas reinhardtii. J. Mol. Biol.* 191:421–432.

Goodenough, U.W. 1989. Cyclic AMP enhances the sexual agglutinability of *Chlamydomonas* flagella. *J. Cell Biol.* 109:247–252.

Goodenough, U.W., B. Shames, L. Small, T. Saito, R.C. Crain, M.A. Sanders, and J.L. Salisbury. 1993. The role of calcium in the *Chlamydomonas reinhardtii* mating reaction. *J. Cell Biol.* 121:365–374.

Hanaoka, K., F. Qian, A. Boletta, A.K. Bhunia, K. Piontek, L. Tsiokas, V.P. Sukhatme, W.B. Guggino, and G.G. Germino. 2000. Co-assembly of polycystin-1 and -2 produces unique cation-permeable currents. *Nature*. 408:990–994.

Harris, E. H. 1989. The *Chlamydomonas* Sourcebook. Academic Press, San Diego. 780 pp.

Hou, Y., H. Qin, J.A. Follit, G.J. Pazour, J.L. Rosenbaum, and G.B. Witman. 2007. Functional analysis of an individual IFT protein: IFT46 is required for transport of outer dynein arms into flagella. *J. Cell Biol.* 176:653–665.

Hu, J., Y.K. Bae, K.M. Knobel, and M.M. Barr. 2006. Casein kinase II and calcineurin modulate TRPP function and ciliary localization. *Mol. Biol. Cell*. 17:2200–2211.

Huang, K., and C.F. Beck. 2003. Phototropin is the blue-light receptor that controls multiple steps in the sexual life cycle of the green alga *Chlamydomonas reinhardtii. Proc. Natl. Acad. Sci. USA*. 100:6269–6274.

Huang, K., T. Merkle, and C.F. Beck. 2002. Isolation and characterization of a *Chlamydomonas* gene that encodes a putative blue-light photoreceptor of the phototropin family. *Physiol. Plant.* 115:613–622.

Iomini, C., V. Babaev-Khaimov, M. Sassaroli, and G. Piperno. 2001. Protein particles in *Chlamydomonas* flagella undergo a transport cycle consisting of four phases. *J. Cell Biol.* 153:13–24.

Jenkins, P.M., T.W. Hurd, L. Zhang, D.P. McEwen, R.L. Brown, B. Margolis, K.J. Verhey, and J.R. Martens. 2006. Ciliary targeting of olfactory CNG channels requires the CNGB1b subunit and the kinesin-2 motor protein, KIF17. *Curr. Biol.* 16:1211–1216.

Kaimori, J.Y., Y. Nagasawa, L.F. Menezes, M.A. Garcia-Gonzalez, J. Deng, E. Imai, L.F. Onuchic, L.M. Guay-Woodford, and G.G. Germino. 2007. Polyductin undergoes notch-like processing and regulated release from primary cilia. *Hum. Mol. Genet.* 16:942–956.

Keller, L.C., E.P. Romijn, I. Zamora, J.R. Yates III, and W.F. Marshall. 2005. Proteomic analysis of isolated *Chlamydomonas* centrioles reveals orthologs of ciliary-disease genes. *Curr. Biol.* 15:1090–1098.

Kiselyov, K., J. Chen, Y. Rbaibi, D. Oberdick, S. Tjon-Kon-Sang, N. Shcheynikov, S. Muallem, and A. Soyombo. 2005. TRP-ML1 is a lysosomal monovalent cation channel that undergoes proteolytic cleavage. *J. Biol. Chem.* 280:43218–43223.

Kottgen, M., T. Benzing, T. Simmen, R. Tauber, B. Buchholz, S. Feliciangeli, T.B. Huber, B. Schermer, A. Kramer-Zucker, K. Hopker, et al. 2005. Trafficking of TRPP2 by PACS proteins represents a novel mechanism of ion channel regulation. *EMBO J.* 24:705–716.

Kozminski, K.G., K.A. Johnson, P. Forscher, and J.L. Rosenbaum. 1993. A motility in the eukaryotic flagellum unrelated to flagellar beating. *Proc. Natl. Acad. Sci. USA*. 90:5519–5523.

Kozminski, K.G., P.L. Beech, and J.L. Rosenbaum. 1995. The *Chlamydomonas* kinesin-like protein FLA10 is involved in motility associated with the flagellar membrane. *J. Cell Biol.* 131:1517–1527.

Lefebvre, P.A., S.A. Nordstrom, J.E. Moulder, and J.L. Rosenbaum. 1978. Flagellar elongation and shortening in *Chlamydomonas*. IV. Effects of flagellar detachment, regeneration, and resorption on the induction of flagellar protein synthesis. *J. Cell Biol.* 78:8–27.

Li, J.B., J.M. Gerdes, C.J. Haycraft, Y. Fan, T.M. Teslovich, H. May-Simera, H. Li, O.E. Blacque, L. Li, C.C. Leitch, et al. 2004. Comparative genomics identifies a flagellar and basal body proteome that includes the BBS5 human disease gene. *Cell*. 117:541–552.

Low, S.H., S. Vasanth, C.H. Larson, S. Mukherjee, N. Sharma, M.T. Kinter, M.E. Kane, T. Obara, and T. Weimbs. 2006. Polycystin-1, STAT6, and P100 function in a pathway that transduces ciliary mechanosensation and is activated in polycystic kidney disease. *Dev. Cell*. 10:57–69.

Luo, Y., P.M. Vassilev, X. Li, Y. Kawanabe, and J. Zhou. 2003. Native polycystin 2 functions as a plasma membrane Ca2+-permeable cation channel in renal epithelia. *Mol. Cell. Biol.* 23:2600–2607.

Martin, N.C., and U.W. Goodenough. 1975. Gametic differentiation in *Chlamydomonas reinhardtii*. I. Production of gametes and their fine structure. *J. Cell Biol.* 67:587–605.

Miedel, M.T., K.M. Weixel, J.R. Bruns, L.M. Traub, and O.A. Weisz. 2006. Posttranslational cleavage and adaptor protein complex-dependent trafficking of mucolipin-1. *J. Biol. Chem.* 281:12751–12759.

Mochizuki, T., G. Wu, T. Hayashi, S.L. Xenophontos, B. Veldhuisen, J.J. Saris, D.M. Reynolds, Y. Cai, P.A. Gabow, A. Pierides, et al. 1996. PKD2, a gene for polycystic kidney disease that encodes an integral membrane protein. *Science*. 272:1339–1342.

Montalbetti, N., Q. Li, Y. Wu, X.Z. Chen, and H.F. Cantiello. 2007. Polycystin-2 cation channel function in the human syncytiotrophoblast is regulated by microtubular structures. *J. Physiol.* 579:717–728.

Montell, C. 2005. The TRP superfamily of cation channels. *Sci. STKE*. 2005:re3.

Moyer, J.H., M.J. Lee-Tischler, H.Y. Kwon, J.J. Schrick, E.D. Avner, W.E. Sweeney, V.L. Godfrey, N.L. Cacheiro, J.E. Wilkinson, and R.P. Woychik. 1994. Candidate gene associated with a mutation causing recessive polycystic kidney disease in mice. *Science*. 264:1329–1333.

Nakayama, T., M. Hattori, K. Uchida, T. Nakamura, Y. Tateishi, H. Bannai, M. Iwai, T. Michikawa, T. Inoue, and K. Mikoshiba. 2004. The regulatory domain of the inositol 1,4,5-trisphosphate receptor is necessary to keep

the channel domain closed: possible physiological significance of specific cleavage by caspase 3. *Biochem. J.* 377:299–307.

Nauli, S.M., F.J. Alenghat, Y. Luo, E. Williams, P. Vassilev, X. Li, A.E. Elia, W. Lu, E.M. Brown, S.J. Quinn, et al. 2003. Polycystins 1 and 2 mediate mechanosensation in the primary cilium of kidney cells. *Nat. Genet.* 33:129–137.

Neill, A.T., G.W. Moy, and V.D. Vacquier. 2004. Polycystin-2 associates with the polycystin-1 homolog, suREJ3, and localizes to the acrosomal region of sea urchin spermatozoa. *Mol. Reprod. Dev.* 67:472–477.

Ong, A.C., and P.C. Harris. 2005. Molecular pathogenesis of ADPKD: the polycystin complex gets complex. *Kidney Int.* 67:1234–1247.

Palmer, C.P., E. Aydar, and M.B. Djamgoz. 2005. A microbial TRP-like polycystic-kidney-disease-related ion channel gene. *Biochem. J.* 387:211–219.

Pan, J., and W.J. Snell. 2000. Signal transduction during fertilization in the unicellular green alga, *Chlamydomonas*. *Curr. Opin. Microbiol.* 3:596–602.

Pan, J., and W.J. Snell. 2002. Kinesin-II is required for flagellar sensory transduction during fertilization in *Chlamydomonas. Mol. Biol. Cell*. 13:1417–1426.

Pan, J., and W.J. Snell. 2005. *Chlamydomonas* shortens its flagella by activating axonemal disassembly, stimulating IFT particle trafficking, and blocking anterograde cargo loading. *Dev. Cell*. 9:431–438.

Pan, J., Q. Wang, and W.J. Snell. 2005. Cilium-generated signaling and cilia-related disorders. *Lab. Invest.* 85:452–463.

Pasquale, S.M., and U.W. Goodenough. 1987. Cyclic AMP functions as a primary sexual signal in gametes of *Chlamydomonas reinhardtii. J. Cell Biol.* 105:2279–2292.

Pazour, G.J., B.L. Dickert, Y. Vucica, E.S. Seeley, J.L. Rosenbaum, G.B. Witman, and D.G. Cole. 2000. *Chlamydomonas* IFT88 and its mouse homologue, polycystic kidney disease gene tg737, are required for assembly of cilia and flagella. *J. Cell Biol.* 151:709–718.

Pazour, G.J., J.T. San Agustin, J.A. Follit, J.L. Rosenbaum, and G.B. Witman. 2002. Polycystin-2 localizes to kidney cilia and the ciliary level is elevated in orpk mice with polycystic kidney disease. *Curr. Biol.* 12:R378–R380.

Pazour, G.J., N. Agrin, J. Leszyk, and G.B. Witman. 2005. Proteomic analysis of a eukaryotic cilium. *J. Cell Biol.* 170:103–113.

Peden, E.M., and M.M. Barr. 2005. The *KLP-6* kinesin is required for male mating behaviors and polycystin localization in *Caenorhabditis elegans. Curr. Biol.* 15:394–404.

Pedersen, L.B., S. Geimer, R.D. Sloboda, and J.L. Rosenbaum. 2003. The Microtubule plus end-tracking protein EB1 is localized to the flagellar tip and basal bodies in *Chlamydomonas reinhardtii. Curr. Biol.* 13:1969–1974.

Praetorius, H.A., and K.R. Spring. 2001. Bending the MDCK cell primary cilium increases intracellular calcium. *J. Membr. Biol.* 184:71–79.

Qian, F., A. Boletta, A.K. Bhunia, H. Xu, L. Liu, A.K. Ahrabi, T.J. Watnick, F. Zhou, and G.G. Germino. 2002. Cleavage of polycystin-1 requires the receptor for egg jelly domain and is disrupted by human autosomal-dominant polycystic kidney disease 1-associated mutations. *Proc. Natl. Acad. Sci. USA*. 99:16981–16986.

Qin, H., J.L. Rosenbaum, and M.M. Barr. 2001. An autosomal recessive polycystic kidney disease gene homolog is involved in intraflagellar transport in *C. elegans* ciliated sensory neurons. *Curr. Biol.* 11:457–461.

Qin, H., D.R. Diener, S. Geimer, D.G. Cole, and J.L. Rosenbaum. 2004. Intraflagellar transport (IFT) cargo: IFT transports flagellar precursors to the tip and turnover products to the cell body. *J. Cell Biol.* 164:255–266.

Qin, H., D.T. Burnette, Y.K. Bae, P. Forscher, M.M. Barr, and J.L. Rosenbaum. 2005. Intraflagellar transport is required for the vectorial movement of TRPV channels in the ciliary membrane. *Curr. Biol.* 15:1695–1699.

Quarmby, L.M. 1994. Signal transduction in the sexual life of *Chlamydomonas*. *Plant Mol. Biol.* 26:1271–1287.

Rosenbaum, J.L., and G.B. Witman. 2002. Intraflagellar transport. *Nat. Rev. Mol. Cell Biol.* 3:813–825.

Scholey, J.M. 2003. Intraflagellar transport. *Annu. Rev. Cell Dev. Biol.* 19:423–443.

Schroda, M., O. Vallon, F.A. Wollman, and C.F. Beck. 1999. A chloroplast-targeted heat shock protein 70 (HSP70) contributes to the photoprotection and repair of photosystem II during and after photoinhibition. *Plant Cell*. 11:1165–1178.

Sizova, I., M. Fuhrmann, and P. Hegemann. 2001. A *Streptomyces rimosus aph-VIII* gene coding for a new type phosphotransferase provides stable antibiotic resistance to *Chlamydomonas reinhardtii. Gene*. 277:221–229.

Snell, W.J., M. Buchanan, and A. Clausell. 1982. Lidocaine reversibly inhibits fertilization in *Chlamydomonas*: a possible role for calcium in sexual signalling. *J. Cell Biol.* 94:607–612.

Sun, Z., A. Amsterdam, G.J. Pazour, D.G. Cole, M.S. Miller, and N. Hopkins. 2004. A genetic screen in zebrafish identifies cilia genes as a principal cause of cystic kidney. *Development*. 131:4085–4093.

Torres, V.E., and P.C. Harris. 2006. Mechanisms of disease: autosomal dominant and recessive polycystic kidney diseases. *Nat. Clin. Pract. Nephrol.* 2:40–55.

Tsiokas, L., T. Arnould, C. Zhu, E. Kim, G. Walz, and V.P. Sukhatme. 1999. Specific association of the gene product of PKD2 with the TRPC1 channel. *Proc. Natl. Acad. Sci. USA*. 96:3934–3939.

Tsiokas, L., S. Kim, and E.C. Ong. 2007. Cell biology of polycystin-2. *Cell. Signal.* 19:444–453.

Venglarik, C.J., Z. Gao, and X. Lu. 2004. Evolutionary conservation of *Drosophila* polycystin-2 as a calcium-activated cation channel. *J. Am. Soc. Nephrol.* 15:1168–1177.

von Gromoff, E.D., U. Treier, and C.F. Beck. 1989. Three light-inducible heat shock genes of *Chlamydomonas reinhardtii. Mol. Cell. Biol.* 9:3911–3918.

Wang, Q., and W.J. Snell. 2003. Flagellar adhesion between mating type plus and mating type minus gametes activates a flagellar protein-tyrosine kinase during fertilization in *Chlamydomonas. J. Biol. Chem.* 278:32936–32942.

Wang, Q., J. Pan, and W.J. Snell. 2006. Intraflagellar transport particles participate directly in cilium-generated signaling in *Chlamydomonas. Cell*. 125:549–562.

Watnick, T.J., Y. Jin, E. Matunis, M.J. Kernan, and C. Montell. 2003. A flagellar polycystin-2 homolog required for male fertility in *Drosophila. Curr. Biol.* 13:2179–2184.

Witman, G.B., K. Carlson, J. Berliner, and J.L. Rosenbaum. 1972. *Chlamydomonas* flagella. I. Isolation and electrophoretic analysis of microtubules, matrix, membranes, and mastigonemes. *J. Cell Biol.* 54:507–539.

Wu, Y., X.Q. Dai, Q. Li, C.X. Chen, W. Mai, Z. Hussain, W. Long, N. Montalbetti, G. Li, R. Glynne, et al. 2006. Kinesin-2 mediates physical and functional interactions between polycystin-2 and fibrocystin. *Hum. Mol. Genet.* 15:3280–3292.

Yoder, B.K., X. Hou, and L.M. Guay-Woodford. 2002. The polycystic kidney disease proteins, polycystin-1, polycystin-2, polaris, and cystin, are co-localized in renal cilia. *J. Am. Soc. Nephrol.* 13:2508–2516.